Electronic Supplementary Material (ESI) for Chemical Science

Lanthanide hexafluoroacetylacetonates versus nitrates for the controlled loading of luminescent polynuclear single-stranded oligomers.

Amir Zaïm, Natalia Dalla Favera, Laure Guénée, Homayoun Nozary, Thi Nhu Y Hoang, Svetlana V. Eliseeva, Stéphane Petoud and Claude Piguet*

Supporting Information (71 pages)

Appendix 1: **Geometrical analysis of the Eu(III) coordination spheres in $[Eu_3(L4)(hfac)_9]$**

Each Eu^{III} cation in $[Eu_3(\mathbf{L4})(hfac)_9]$ is nine-coordinated by the three donor atoms of the tridentate aromatic binding segment of **L4** and by six oxygen atoms of three didentate hexafluoroacetylacetonate anions. In each coordination sphere, the donor atoms occupy the vertices of a distorted polyhedron, which is usually analyzed as a distorted monocapped square antiprism for ternary complexes $[Ln(\mathbf{L})(hfac)_3]$, where **L** is a tridentate neutral ligand.[S1] When different geometries are to be compared, the use of the famous *S* angle of the 'shape measure' parameter is pertinent,[S2] but it is of more limited interest for characterizing a single set of analogous structures, and we therefore resort to the vectorial shape analysis proposed by LeBorgne et al.[S3] Following this approach, each coordination sphere of Eu(III) can be described as a distorted monocapped square antiprism (MSA), in which O3, O4, O5, O6 and O1, O3, N2, N8 for the central EuN_3O_6 unit (Figure S11a), and O13, O15, O17, O18 and O2, O14, O16, N10 for the distal EuN_2O_7 unit (Figure S11b) define, respectively, the lower and the upper tetragonal faces of the approximate antiprism, the latter being capped by N1 (EuN_3O_6 unit) or by N12 (EuN_2O_7 unit). The computed resulting vector *R*1 (resp. *R*2) corresponds to the sum of the four Eu-donor atoms vectors forming the upper (resp. the lower) tetragonal face of the antiprism. The θ angles between each generating upper Eu-donor vector and *R*1 (resp between each lower Eu-donor vector and *R*2), measure the flatening of the antiprism along the pseudo-C_4 axis defined by the *R*1-*R*2 direction (EuN_3O_6 unit: $34.7 \leq \theta \leq 68.7°$, average 66(5)°for the upper face and 50(15)° for the lower face in Table S4; EuN_2O_7 unit: $51.0 \leq \theta \leq 70.2°$, average 65(4)°for the upper face and 54(3)° for the lower face in Table S5), whereas the ϕ angle (EuN_3O_6 unit: 175.4°; EuN_2O_7 unit: 177.8°) between *R1* and *R*2 indicates a minor bending of the two tetragonal faces ($\phi = 180°$ in an ideal MSA, Tables S2-S3). The rather broad distribution of θ_i suggests some significant distortions from the idealized Johnson capped square antiprism[S4] despite a rather regular distribution of the ω_i angles between the projected vectors of the tetrapodes along the pseudo-C_4 axis (EuN_3O_6 unit: average ω(intra-tetrapode) = 90(10)°, ideal: 90° and average ω(inter-tetrapode) = 45(7)° in Table S4; EuN_2O_7 unit: average

ω(intra-tetrapode) = 90(4)°, ideal: 90° and average ω(inter-tetrapode) = 45(3)° in Table S5) together with a minor deviation of the capping N(pyridine) atom from the pseudo-C_4 axis (EuN_3O_6 unit: α = 2.5°; EuN_2O_7 unit: α = 2.3°). According that all Eu-O and Eu-N bonds are comparable, vector normalization to unit length[S3] does not significantly affect the geometrical analysis (Tables S3-S4). A more rigorous analysis of the coordination sphere of nine-coordinate metal complexes based on the spherical relaxation of the five Johnson polyhedra possessing nine vertices[S4] shows that the distorted central EuN_3O_6 coordination sphere in [Eu_3(**L4**)(hfac)$_9$] can be alternatively described as a 2:5:2 hula hoop (HH), in which the basal plane is defined by N1, N2, N8, O5, O6 related by a five-fold pseudo-symmetry axis with two vertices (O1, O2) and (O3,O4), each related by a two-fold pseudo-symmetry axis, and located on each opposite side of the central pentagone (Fig. S11a).[S9] On the contrary, the less distorted distal EuN_2O_7 coordination spheres in [Eu_3(**L4**)(hfac)$_9$] do not fit this criteria (Fig. S11b).

References

[S1] Y. Kuramochi, T. Nakagawa, T. Yokoo, J. Yuasa, T. Kawai, Y. Hasegawa, *Dalton Trans.* **2012**, *41*, 6634-6640.

[S2] (a) B. E. Robertson, *Inorg. Chem.*, **1977**, *16*, 2735–2742. (b) M. C. Favas, D. L. Kepert, *Prog. Inorg. Chem.* **1981**, *28*, 309–367. (c) J. Xu, E. Radkov, M. Ziegler, K. N. Raymond, *Inorg. Chem.* **2000**, 39, 4156–4164. (d) S. V. Eliseeva, O. V. Kotova, F. Gumy, S. N. Semenov, V. G. Kessler, L. S. Lepnev, J.-C. G. Bünzli, N. P. Kuzmina, *J. Phys. Chem. A*, **2008**, *112*, 3614–3614. (e) T. Harada, Y. Nakano, M. Fujiki, M. Naito, T. Kawai, Y. Hasegawa, *Inorg. Chem.* **2009**, *48*, 11242–11250. (f) B. E. Robertson, *Inorg. Chem.*, **1977**, *16*, 2735–2742. (e) M. C. Favas, D. L. Kepert, *Prog. Inorg. Chem.* **1981**, *28*, 309–367.

[S3] T. Le Borgne, J.-M. Bénech, S. Floquet, G. Bernardinelli, C. Aliprandini, P. Bettens, C. Piguet, *Dalton Trans.* **2003**, 3856-3868.

[S4] A. Ruiz-Martinez, D. Casanova, S. Alvarez, *Chem. Eur. J.* **2008**, *14*, 1291-1303.

Appendix 2: **Geometrical analysis of the helicity in $[Eu_2(L3)(hfac)_6]$, $[Lu_2(L3)(hfac)_6]$ and $[Eu_3(L4)(hfac)_9]$**

We have resorted to the detailed analysis of crooked lines proposed by Brewster[30] for the quantitative determination of the helicity index *H* (eqn S1) associated with the specific organization of the five-carbon chain HC_{ar}-C_{ar}-CH_2-C_{ar}-$C_{ar}H$ in the spacer and numbered C15-C14-C20-C21-C27 in $[Eu_2(\mathbf{L3})(hfac)_6]$ (Figure S2a).

$$H = \frac{V}{V_{max}} = 6\sqrt{3}\pi\frac{L \cdot A}{D^3} \qquad \text{(S1)}$$

According to Brewster,[30] the five atoms are projected onto a plane perpendicular to the helical axis defined by the line passing through the two terminal atoms of the chain. This yields three possible geometrical figures: a line for non-helical organization, a quadrilateral for a regular helical crooked line and two triangles with a common summit for an amphiverse helix.[19] The helicity index computed with eqn (S1) corresponds to the ratio of the volume enclosed by the crooked line (V) with respect to the maximum volume (V_{max}) produced when the subtended figure is a circle (L is the end to end distance of the helix, A is the area of the subtended figure in the projection plane and D is the total length of the crooked line, Figure S12a).[30] For $[Eu_2(\mathbf{L3})(hfac)_6]$, $[Lu_2(\mathbf{L3})(hfac)_6]$ and $[Eu_3(\mathbf{L4})(hfac)_9]$, the subtended figures produced by the crooked line of the diphenylmethane spacers are diagnostic for the existence of regular helices (Figure S12b). The introduction of the geometrical data gathered in Table S21 into eqn (S1) gives helicity indexes of H = 0.52 ($[Eu_2(\mathbf{L3})(hfac)_6]$), H = 0.58 ($[Lu_2(\mathbf{L3})(hfac)_6]$) and H = 0.71, 0.83 ($[Eu_3(\mathbf{L4})(hfac)_9]$).

Appendix 3. **Correction of the rough spectrophotometric data for the residual absorption of [Ln(hfac)$_3$]**.

For a given stoichiometric ratio $x = \left|\mathrm{Ln}\right|_{\mathrm{tot}} / \left|\mathbf{L}\boldsymbol{k}\right|_{\mathrm{tot}}$, the absorbance A_x^{λ} recorded at the wavelength λ for a mixture produced by equilibrium (2) can be expressed with the Lambert-Beer relationship (eq S2, l is the pathlength of the incident light within the solution, ε_i^{λ} is the molar absorption coefficient of species i at the wavelength λ).

$$\frac{A_x^{\lambda}}{l} = \varepsilon_{\mathrm{Ln(hfac)_3}}^{\lambda} \left|\mathrm{Ln(hfac)_3}\right| + \varepsilon_{\mathrm{Lk}}^{\lambda} \left|\mathbf{L}\boldsymbol{k}\right| + \varepsilon_{\mathrm{Ln\text{-}Lk}}^{\lambda} \left|\mathrm{Ln}(\mathbf{L}\boldsymbol{k})\mathrm{(hfac)_3}\right| \qquad \text{(S2)}$$

The introduction of the mass balances given in eqs (S3)-(S4) into eq (S2) yields eq (S5), which can be easily rearranged to give eq (S6).

$$\left|\mathrm{Ln}\right|_{\mathrm{tot}} = \left|\mathrm{Ln(hfac)_3}\right| + \left|\mathrm{Ln}(\mathbf{L}\boldsymbol{k})\mathrm{(hfac)_3}\right| \qquad \text{(S3)}$$

$$\left|\mathbf{L}\boldsymbol{k}\right|_{\mathrm{tot}} = \left|\mathbf{L}\boldsymbol{k}\right| + \left|\mathrm{Ln}(\mathbf{L}\boldsymbol{k})\mathrm{(hfac)_3}\right| \qquad \text{(S4)}$$

$$\frac{A_x^{\lambda}}{l} = \varepsilon_{\mathrm{Ln(hfac)_3}}^{\lambda} \left(\left|\mathrm{Ln}\right|_{\mathrm{tot}} - \left|\mathrm{Ln}(\mathbf{L}\boldsymbol{k})\mathrm{(hfac)_3}\right|\right) + \varepsilon_{\mathrm{Lk}}^{\lambda} \left(\left|\mathbf{L}\boldsymbol{k}\right|_{\mathrm{tot}} - \left|\mathrm{Ln}(\mathbf{L}\boldsymbol{k})\mathrm{(hfac)_3}\right|\right) + \varepsilon_{\mathrm{Ln\text{-}Lk}}^{\lambda} \left|\mathrm{Ln}(\mathbf{L}\boldsymbol{k})\mathrm{(hfac)_3}\right| \qquad \text{(S5)}$$

$$F\left(\lambda, \left|\mathrm{Ln}\right|_{\mathrm{tot}}, \left|\mathbf{L}\boldsymbol{k}\right|_{\mathrm{tot}}\right) = \frac{A_x^{\lambda}}{l\left|\mathbf{L}\boldsymbol{k}\right|_{\mathrm{tot}}} - \varepsilon_{\mathrm{Ln(hfac)_3}}^{\lambda} \left(\frac{\left|\mathrm{Ln}\right|_{\mathrm{tot}}}{\left|\mathbf{L}\boldsymbol{k}\right|_{\mathrm{tot}}}\right) = \varepsilon_{\mathrm{Lk}}^{\lambda} + \frac{\left(\varepsilon_{\mathrm{Ln\text{-}Lk}}^{\lambda} - \varepsilon_{\mathrm{Lk}}^{\lambda} - \varepsilon_{\mathrm{Ln(hfac)_3}}^{\lambda}\right)}{\left|\mathbf{L}\boldsymbol{k}\right|_{\mathrm{tot}}} \left|\mathrm{Ln}(\mathbf{L}\boldsymbol{k})\mathrm{(hfac)_3}\right| \qquad \text{(S6)}$$

During the spectrophotometric titration, $F\left(\lambda, \left|\mathrm{Ln}\right|_{\mathrm{tot}}, \left|\mathbf{L}\boldsymbol{k}\right|_{\mathrm{tot}}\right)$ is a constant at a specific wavelength λ_0 for which $\left(\varepsilon_{\mathrm{Ln\text{-}Lk}}^{\lambda_0} - \varepsilon_{\mathrm{Lk}}^{\lambda_0} - \varepsilon_{\mathrm{Ln(hfac)_3}}^{\lambda_0}\right) = 0$. This condition has non-negligible probability to occur only for the formation of a single additional absorbing complex. We also note that any graphical representation of $F\left(\lambda, \left|\mathrm{Ln}\right|_{\mathrm{tot}}, \left|\mathbf{L}\boldsymbol{k}\right|_{\mathrm{tot}}\right)$ as a function of $1/\left|\mathbf{L}\boldsymbol{k}\right|_{\mathrm{tot}}$ becomes linear after the final end point of the titration.

Appendix 4. **Calculation of the binding isotherm in polymer 1**.[12,13]

Let us write the multiple intermolecular complexation process depicted in Fig. 1a between receptor (ligand) **L** and metals M with equilibrium S7.

$$\mathbf{L} + m\,\mathrm{M}^{z+} \rightleftharpoons [\mathbf{L}\mathrm{M}_m]^{mz+} \qquad \beta_{m,1}^{\mathrm{M},\mathbf{L}} \tag{S7}$$

Each macrospecies $[\mathbf{L}\mathrm{M}_m]^{mz+}$ is made up of several microspecies differing in the exact location of the m metals bound to the N sites ($m \le N$). Each microspecies $\{\boldsymbol{s}_\mathrm{i}\}$-$[\mathbf{L}\mathrm{M}_m]^{mz+}$ can be thus defined by a state vector $\{\boldsymbol{s}_\mathrm{i}\}$, for which each element $s_\mathrm{i} = 1$ when a metal is bound to site i and $s_\mathrm{i} = 0$ when no metal is coordinated. The free energy of complexation $G\{\boldsymbol{s}_\mathrm{i}\}$ associated with the formation of the microspecies $\{\boldsymbol{s}_\mathrm{i}\}$-$[\mathbf{L}\mathrm{M}_m]^{mz+}$ is given in eq S8, where the first term linear in the state variable s_i, corresponds to the sum of free energies of intermolecular metal-binding site connections, and the second quadratic term estimates the sum of the intermetallic pairs interactions limited to nearest neighbours.

$$G\left(\{\boldsymbol{s}_i\}\right) = -\sum_{i=1}^{N} RT \ln\left(f_i^{\mathrm{M}}\right) s_i + \frac{1}{2}\sum_{i=1}^{N}\sum_{j\neq i}^{N} \Delta E_{i,j}^{\mathrm{M},\mathrm{M}} s_i s_j \tag{S8}$$

The associated microscopic formation constant is obtained by the van't Hoff isotherm $\beta_{m,1}^{\mathrm{M},\mathbf{L}}\left(\{\boldsymbol{s}_i\}\right) = \exp\left[-G\left(\{\boldsymbol{s}_i\}\right)/RT\right]$, and the target macroconstant in equilibrium S7 is simply obtained by the sum over all contributing microconstants.

$$\beta_{m,1}^{\mathrm{M},\mathbf{L}} = \sum_{\{\boldsymbol{s}_i\}} \beta_{m,1}^{\mathrm{M},\mathbf{L}}\left(\{\boldsymbol{s}_i\}\right) = \sum_{\{\boldsymbol{s}_i\}} \exp\left[-G_{m,1}^{\mathrm{M},\mathbf{L}}\left(\{\boldsymbol{s}_i\}\right)/RT\right] \tag{S9}$$

The relevant information on the binding properties of M to **L** is contained in the semi-grand partition function Ξ, which is equivalent to the so-called binding polynomial of eq S10, where a_M is the activity of the free metal ion.

$$\Xi = \sum_{m=0}^{N} \beta_{m,1}^{\mathrm{M},\mathbf{L}} \left(a_\mathrm{M}\right)^m \tag{S10}$$

The degree of metalation $\theta_\mathrm{M} = \langle m \rangle / N$, also known in coordination chemistry as the occupancy factor estimating the average of bound metals per receptor, is given by eq S11.

$$\theta_\mathrm{M} = \frac{\langle m \rangle}{N} = \frac{1}{N}\frac{\left|\mathrm{M}_\mathrm{bound}\right|}{\left|\mathbf{L}_\mathrm{tot}\right|} = \frac{1}{N}\frac{d\ln(\Xi)}{d\ln\left(a_\mathrm{M}\right)} \tag{S11}$$

Introducing eq S10 into eq S11, followed by derivation eventually yields

$$\theta_\mathrm{M} = \frac{1}{N}\frac{\sum_{m=0}^{N} m\beta_{m,1}^{\mathrm{M},\mathbf{L}}\left(a_\mathrm{M}\right)^m}{\Xi} = \frac{1}{N}\frac{\sum_{m=0}^{N} m\beta_{m,1}^{\mathrm{M},\mathbf{L}}\left(a_\mathrm{M}\right)^m}{\sum_{m=0}^{N} \beta_{m,1}^{\mathrm{M},\mathbf{L}}\left(a_\mathrm{M}\right)^m} \tag{S12}$$

We note that this approach is not limited to occupancy factors (eq S11), and any alternative techniques, which estimate the semi-grand partition function Ξ for various metal activities, can be

used for deducing the macroconstants (eq S10). For instance, the partition function for the entire chain with N sites shown in Fig. 1a can be computed by suming the elements of the partition vector of the elementary subchain over all possible values of the site variables. This operation can be formulated in matrix notation in eq S13, whereby $\mathrm{V_g}$ is the generating vector initiating the effect of the transfer matrix **T**, which takes into account the change produced in the partition vector when the subchain is extended by one elementary unit on the left. $\tilde{\mathrm{V}}_\mathrm{t}$ is the transposed terminating vector.

$$\Xi = \tilde{\mathrm{V}}_\mathrm{t}\, \mathbf{T}^N\, \mathrm{V}_g \qquad \text{(S13)}$$

For infinite long chains considered in polymers ($N \to \infty$), the partition function is given by $\Xi \sim \lambda^N$, where λ is the largest eigenvalue of the transfer matrix **T**. The transfer matrix adapted to a finite chain with vicinal and distal intermetallic interactions between lanthanides for even N values is shown below and the partition functions can be deduced for N = 8 by using eq S13 with $\tilde{\mathrm{V}}_\mathrm{g} = (1,0,0,0,0,0,0,0)$ and $\tilde{\mathrm{V}}_\mathrm{t} = (1,1,1,1,1,1,1,1)$, whereas the target occupancy factor are obtained by derivation with eq S11.

a)

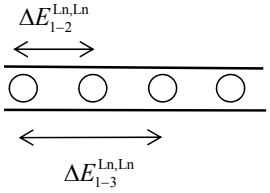

b)

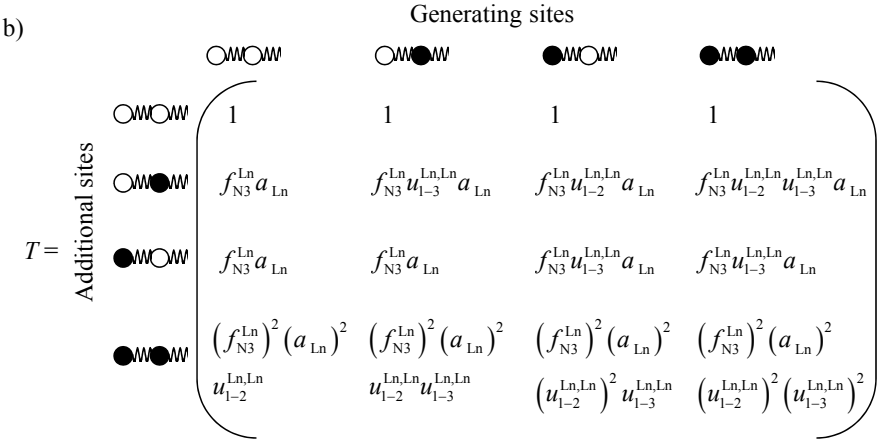

Figure S0 a) Schematic illustration of vicinal $\Delta E_{1\text{-}2}^{\mathrm{Ln,Ln}}$ and distal $\Delta E_{1\text{-}3}^{\mathrm{Ln,Ln}}$ intermetallic pair interactions operating along a linear metal-loaded receptor and b) associated transfer matrix (o = empty site, ● = occupied site) for even N values.[12,13]

Introducing $\Delta G_{\mathrm{inter}}^{\mathrm{Ln,N_3}} = -RT \ln\left(f_{\mathrm{N_3}}^{\mathrm{Ln}}\right)$, $\Delta E_{1\text{-}2}^{\mathrm{Ln,Ln}}$ and $\Delta E_{1\text{-}3}^{\mathrm{Ln,Ln}}$ collected in Tables S29-S30 into the transfer matrix of Fig S0b eventually yields the occupancy factors plotted with respect to the activity of the free metal, thus leading to the so-called binding isotherms depicted in Figure 10.

Table S1 Elemental Analyses for $[Ln_m(\mathbf{L}k)(hfac)_{3m}]$ complexes (k = 2, 3, 4; Ln = La, Eu, Gd, Lu).

Compounds	MM/ g·mol^{-1}	%C found	%H found	%N found	%C calc	%H calc	%N calc
$[La(\mathbf{L2})_2(hfac)_2]_2$ $[La_2(hfac)_4(O_2CCF_3)_4]\cdot 2.4\ H_2O$	1976.86	37.26	2.52	5.57	37.67	2.45	5.67
$[Eu(\mathbf{L2})(hfac)_3]$	1095.52	37.23	2.35	5.13	37.28	2.30	5.11
$[Gd(\mathbf{L2})(hfac)_3]$	1100.81	37.19	2.34	4.94	37.09	2.29	5.09
$[Lu(\mathbf{L2})(hfac)_3]$	1118.53	36.45	2.31	5.08	36.51	2.25	5.01
$[Eu_2(\mathbf{L3})(hfac)_6].1.1\ H_2O$	2203.06	37.26	2.31	5.01	37.62	2.29	5.09
$[Gd_2(\mathbf{L3})(hfac)_6].1.2\ H_2O$	2213.64	37.06	2.36	5.11	37.44	2.28	5.06
$[Lu_2(\mathbf{L3})(hfac)_6].0.5\ H_2O$	2249.06	36.71	2.27	4.96	36.85	2.24	4.98
$[Eu_3(\mathbf{L4})(hfa)_9].1.4\ H_2O$	3355.64	38.39	2.28	5.15	38.66	2.22	5.43
$[Gd_3(\mathbf{L4})(hfa)_9]$	3371.50	38.58	2.42	5.22	38.47	2.21	5.40

Table S2 Summary of crystal data, intensity measurements and structure refinements for [Eu(**L2**)(hfac)$_3$] (**2**), [Lu(**L2**)(hfac)$_3$] (**5**), [Eu$_2$(**L3**)(hfac)$_6$] (**3**), [Lu$_2$(**L3**)(hfac)$_6$] (**6**) , [Eu$_3$(**L4**)(hfa)$_9$]·5.5CH$_3$CN (**4**).

	[Eu(**L2**)(hfac)$_3$] (**2**)	[Lu(**L2**)(hfac)$_3$] (**5**)	[Eu$_2$(**L3**)(hfac)$_6$] (**3**)	[Lu$_2$(**L3**)(hfac)$_6$] (**6**)[a]	[Eu$_3$(**L4**)(hfac)$_9$] (**4**)
Empirical formula	$C_{34}H_{25}F_{18}N_4O_7Eu$	$C_{38}H_{31}F_{18}N_6O_7Lu$	$C_{69}H_{50}F_{36}N_8O_{14}Eu_2$	$C_{69}H_{50}F_{36}N_8O_{14}\ Lu_2$	$C_{119}H_{90.5}F_{54}N_{18.5}O_{20}Eu_3$
Formula weight	1095.54	1200.66	2203.09	2249.11	3581.48
Temperature	180 (2) K	180(2) K	180(2) K	180(2) K	180(2) K
Wavelength	0.71073 Å	1.54184 Å	0.71073 Å	1.54184 Å	1.54184 Å
Crystal System, Space group	Monoclinic, $P2_1/c$	Triclinic, P-1	Monoclinic, $P2_1/c$	Triclinic, P-1	Triclinic, P-1
Unit cell dimensions	a = 12.4834 (1) Å	a = 12.2354 (2) Å	a = 21.9162 (8) Å	a = 12.6357 (4) Å	a = 17.6614 (4) Å
	b = 18.5861 (2) Å	b = 14.4044 (2) Å	b = 18.3619 (8) Å	b = 17.6457 (5) Å	b = 19.7308 (4) Å
	c = 20.5491 (3) Å	c = 14.8029 (3) Å	c = 24.8681 (9) Å	c = 18.3732 (6) Å	c = 23.4654 (5) Å
	α = 90°	α = 77.3039 (16)°	α = 90°	α = 83.577 (3)°	α = 95.2886 (19)°
	β = 117.5470 (10)°	β = 72.1925 (19)°	β = 122.872 (2)°	β = 89.254 (3)°	β = 96.6780 (19)°
	γ = 90°	γ = 68.6551 (17)°	γ = 90°	γ = 88.667 (2)°	γ = 114.691 (2)°
Volume in Å^3	4227.24 (8)	2296.18 (8)	8405.1 (6)	4069.6 (2)	7288.7 (3)
Z, Calculated density	4, 1.721 Mg/m^3	2, 1.737 Mg/m^3	4, 1.741 Mg/m^3	2, 1.835 Mg/m^3	2, 1.632 Mg/m^3
Absorption coefficient	1.612 mm^{-1}	5.275 mm^{-1}	1.622 mm^{-1}	5.888 mm^{-1}	10.343 mm^{-1}
F(000)	2152	1180	4328	2196	3538
Theta range for data collection	1.98 to 29.59°	3.16 to 73.39 °	1.48 to 25.71°	2.52 to 79.77 °	2.79 to 73.46 °

Table S2 (continued)

Limiting indices	-15<=*h*<=17,	-14<=*h*<=15,	-26<=*h*<=26,	-15<=*h*<=15,	-16<=*h*<=21,
	-23<=*k*<=25,	-17<=*k*<=17,	-22<=*k*<=22,	-21<=*k*<=21,	-24<=*k*<=20,
	-26<=*l*<=25	-18<=*l*<=18	-30<=*l*<=30	-22<=*l*<=22	-29<=*l*<=26
Reflections collected / unique	70644 / 10864	34152 / 9099	74386 / 15887	24565 / 24565	53489 / 28544
	[*R*(int) = 0.0311]	[*R*(int) = 0.0283]	[*R*(int) = 0.0976]	[*R*(int) = 0.0000]	[*R*(int) = 0.0398]
Completeness to theta	26.32°/ 99.9 %	73.39°/ 98.4%	25.71°/ 99.2%	68.00°/ 99.2 %	66.97°/ 99.9 %
Data / restraints / parameters	10864 / 12 / 573	9099 / 0 / 634	15887 / 34 / 1132	24565 / 18 / 1143	28544 / 2 / 1894
Goodness-of-fit on F^2	1.049	1.037	1.027	1.020	1.046
Final *R* indices [$I>2\sigma(I)$]	R_1 = 0.0412,	R_1 = 0.0264,	R_1 = 0.0640,	R_1 = 0.0606,	R_1 = 0.0567,
	ωR_2 = 0.1059	ωR_2 = 0.0693	ωR_2 = 0.1592	ωR_2 = 0.1655	ωR_2 = 0.1455
R indices (all data)	R_1 = 0.0504,	R_1 = 0.0277,	R_1 = 0.0863,	R_1 = 0.0694,	R_1 = 0.0715,
	ωR_2 = 0.1150	ωR_2 = 0.0704	ωR_2 = 0.1708	ωR_2 = 0.1742	ωR_2 = 0.1585
Largest diff. peak and hole	1.827 and -1.108 e.Å^{-3}	0.801 and -0.526 e.Å^{-3}	1.391 and -1.385 e.Å^{-3}	1.785 and -1.463 e.Å^{-3}	1.328 and -1.342 e.Å^{-3}

[a] The crystal is a non merohedral twin, the ratio of the twin components beign 0.47:0.53. The structure refinement was performed using HKLF 5 Shelx reflection file

Table S3 Ionic radius (R_{Ln}),[a] average bond valences ($\nu_{Ln,j}$),[b] bond valence sums ($V_{Ln,j}$)[c] and rotation (α) and nutation (β) angles[d] in the crystal structures of $[Ln_m(\mathbf{Lk})(hfac)_{3m}]$ and $[Ln_m(\mathbf{Lk})(NO_3)_{3m}]$ (m = 1-3, **Lk** = **L1**-**L4**).

Complexes	Type [e]	R_{Ln}/Å	$\nu_{Ln,N\text{-}py}$	$\nu_{Ln,N\text{-}bzim}$	$\nu_{Ln,O\text{-}amide}$	$\nu_{Ln,O\text{-}hfac}$	$\nu_{Ln,O\text{-}NO3}$	V_{Ln}	α/°	β/°	Ref.
$[Eu(\mathbf{L1})(hfac)_3]$	NNN	1.06	0.33	0.36(1)	-	0.39(4)	-	3.37	40.2	176.8	18
$[Lu(\mathbf{L1})(hfac)_3]$	NNN	1.00	0.25	0.340(2)	-	0.35(6)	-	3.00	44.5	180.0	18
$[Eu(\mathbf{L2})(hfac)_3]$	NNO	1.10	0.30	0.34	0.38	0.36(2)	-	3.15	87.9	132.7	This work
$[Lu(\mathbf{L2})(hfac)_3]$	NNO	1.01	0.29	0.30	0.39	0.34(4)	-	3.04	83.6	133.6	This work
$[Eu(\mathbf{L2})(NO_3)_3(CH_3CN)]$	NNO	1.17	0.28	0.36	0.41	-	0.27(2)	2.98	-	-	19
$[Eu_2(\mathbf{L3})(hfac)_6]$	NNO	1.10	0.28(1)	0.322(1)	0.390(4)	0.36(3)	-	3.16(3)	85(3)	134(2)	This work
$[Lu_2(\mathbf{L3})(hfac)_6]$	NNO	1.02	0.31(1)	0.30(2)	0.40(1)	0.34(4)	-	3.02(7)	83(2)	133.8(6)	24
$[Eu_2(\mathbf{L3})(NO_3)_6(H_2O)_2]$	NNO	1.16	0.28	0.39	0.42	-	0.26(3)	2.98	-	-	19
$[Eu_3(\mathbf{L4})(hfac)_9]$	NNN	1.09	0.27	0.36(1)	-	0.36(4)	-	3.13	40.0	176.1	This work
	NNO	1.09	0.30(1)	0.32(2)	0.36(1)	0.36(3)	-	3.11(3)	86(4)	135(4)	This work

[a] Ionic radius for Ln^{III} calculated according to Shannon's definition with r(N) = 1.46 Å, r(O) = 1.35 Å and r(O-nitrate) = 1.31 Å.[28] [b] $\nu_{Ln,j} = e^{\left[\left(R_{Ln,j} - d_{Ln,j}\right)/b\right]}$ with valence bond parameters $R_{Ln,N}$ and $R_{Ln,O}$ taken from ref 29e,f and b = 0.37 Å.[29] [c] $V_{Ln} = \sum_j \nu_{Ln,j}$.[29] [d] α is the interplanar angle between the equatorial didentate hfac anion and the plane defined by the three coordinated donor atom of the aromatic ligand. β is the angle between the Eu-N_{py} and the Eu-O1(hfac)+Eu-O2(hfac) direction (Figure 3). [e] Sequence of donor atoms in the tridentate aromatic ligand.

Table S4 Selected structural data for the Eu1 lanthanide coordination sphere in $[Eu_3(\mathbf{L4})(hfac)_9]$ (**4**).

		Angle ϕ [a] / °	
	EuN_3O_6		Perfect MSA[b]
	Standard	Normalized	
R^1-Eu-R^2	175.4	175.7	180
		Angle α [a] / °	
	EuN_3O_6		Perfect MSA[b]
	Standard	Normalized	
	2.5	2.5	0
		Angles θ_t [a] / °	
	EuN_3O_6		Perfect MSA[b]
	Standard	Normalized	
R^1-Eu-O3	66.0	65.9	ρ
R^1-Eu-O1	70.5	70.6	ρ
R^1-Eu-N2	68.7	68.5	ρ
R^1-Eu-N8	58.5	58.7	ρ
R^2-Eu-O2	64.1	64.1	ρ
R^2-Eu-O4	63.8	63.9	ρ
R^2-Eu-O5	40.6	40.4	ρ
R^2-Eu-N6	34.7	34.9	ρ

		Angles ω_{ij} [a] / °	
	EuN_3O_6		Perfect MSA[b]
	Standard	Normalized	
Proj[N2]-Eu-Proj[O3][c]	80.1	80.1	90
Proj[O3]-Eu-Proj[N8]	98.0	98.0	90
Proj[N8]-Eu-Proj[O1]	75.5	75.5	90
Proj[O1]-Eu-Proj[N2]	106.4	106.4	90
Proj[O2]-Eu-Proj[O5]	95.4	95.5	90
Proj[O5]-Eu-Proj[O4]	90.1	90.2	90
Proj[O4]-Eu-Proj[O6]	85.9	85.9	90
Proj[O6]-Eu-Proj[O2]	88.5	88.5	90
Proj[O2]-Eu-Proj[N2]	54.5	54.5	45

Proj[O2]-Eu-Proj[O1]	51.9	51.8	45
Proj[O5]-Eu-Proj[N2]	40.9	41.0	45
Proj[O5]-Eu-Proj[O3]	39.2	39.2	45
Proj[O4]-Eu-Proj[O3]	51.0	51.0	45
Proj[O4]-Eu-Proj[N8]	47.1	47.0	45
Proj[O6]-Eu-Proj[O1]	36.6	36.7	45
Proj[O6]-Eu-Proj[N8]	38.9	38.9	45

[a] For the definition of ϕ, α, θ_i and ω_{ij}, see Fig. S11a. The error in the angles is typically 0.5°. [b] MSA = monocapped square antiprism. [c] Proj[O*i*] and Proj[N*i*] are the projections of O*i* and respectively N*i* along the R^2-R^1 direction onto a perpendicular plane passing through the lanthanide atom. R^1 = Eu-O1 + Eu-N2 + Eu-O3 + Eu-N8 and R^2 = Eu-O2 + Eu-O4 + Eu-O5 + Eu-O6.

Table S5 Selected structural data for the Eu3 lanthanide coordination sphere in $[Eu_3(\mathbf{L4})(hfac)_9]$ (**4**).

		Angle ϕ [a] / °	
	EuN_2O_7		Perfect MSA[b]
	Standard	Normalized	
R^1-Eu-R^2	177.8	178.8	180
		Angle α [a] / °	
	EuN_3O_6		Perfect MSA[b]
	Standard	Normalized	
	2.3	2.6	0
		Angles θ_t [a] / °	
	EuN_3O_6		Perfect MSA[b]
	Standard	Normalized	
R^1-Eu-O2	64.9	62.8	ρ
R^1-Eu-O14	70.2	69.9	ρ
R^1-Eu-O16	64.9	65.1	ρ
R^1-Eu-N10	60.9	63.0	ρ
R^2-Eu-O13	57.2	56.9	ρ
R^2-Eu-O15	53.1	52.9	ρ
R^2-Eu-O17	51.0	51.2	ρ
R^2-Eu-O18	55.3	55.7	ρ

		Angles ω_{ij} [a] / °	
	EuN_3O_6		Perfect MSA[b]
	Standard	Normalized	
Proj[O2]-Eu-Proj[O14][c]	86.1	86.6	90
Proj[O14]-Eu-Proj[N10]	96.7	96.3	90
Proj[N10]-Eu-Proj[O16]	84.3	84.3	90
Proj[O16]-Eu-Proj[O2]	92.8	92.8	90
Proj[O13]-Eu-Proj[O17]	89.4	89.5	90
Proj[O17]-Eu-Proj[O18]	90.8	89.6	90
Proj[O18]-Eu-Proj[O15]	88.9	88.9	90
Proj[O15]-Eu-Proj[O13]	90.9	92.0	90
Proj[O17]-Eu-Proj[O2]	45.7	45.1	45
Proj[O17]-Eu-Proj[O14]	40.4	41.1	45

Proj[O18]-Eu-Proj[O2]	45.1	44.6	45
Proj[O18]-Eu-Proj[O16]	47.8	48.8	45
Proj[O15]-Eu-Proj[N10]	43.1	43.7	45
Proj[O15]-Eu-Proj[O16]	41.2	40.1	45
Proj[O13]-Eu-Proj[O14]	49.0	48.5	45
Proj[O13]-Eu-Proj[N10]	47.7	48.3	45

---

[a] For the definition of ϕ, α, θ_i and ω_{ij}, see Fig. S11. The error in the angles is typically 0.5°. [b] MSA = monocapped square antiprism. [c] Proj[O*i*] and Proj[N*i*] are the projections of O*i* and respectively N*i* along the R^2-R^1 direction onto a perpendicular plane passing through the lanthanide atom. R^1 = Eu-O2 + Eu-O14 + Eu-O16 + Eu-N10 and R^2 = Eu-O13 + Eu-O15 + Eu-O17 + Eu-O18.

Table S6 Selected bond distances (Å), bond angles (°) in [Eu(**L2**)(hfac)$_3$] (**2**).

Bond distances (Å)

Atom 1	Atom 2	Distance	Atom 1	Atom 2	Distance
Eu(1)	O(1)	2.396(3)	Eu(1)	O(6)	2.421(3)
Eu(1)	O(2)	2.450(3)	Eu(1)	O(7)	2.445(3)
Eu(1)	O(3)	2.417(3)	Eu(1)	N(1)	2.612(3)
Eu(1)	O(4)	2.394(2)	Eu(1)	N(3)	2.566(3)
Eu(1)	O(5)	2.397(2)			

Angles (°)

At. 1	At. 2	At. 3	Angle	At. 1	At. 2	At. 3	Angle
O(1)	Eu(1)	O(2)	70.32(9)	O(4)	Eu(1)	O(6)	77.51(9)
O(1)	Eu(1)	O(3)	75.48(10)	O(4)	Eu(1)	O(7)	147.64(9)
O(1)	Eu(1)	O(5)	81.63(9)	O(4)	Eu(1)	N(1)	128.83(9)
O(1)	Eu(1)	O(6)	136.29(9)	O(4)	Eu(1)	N(3)	79.33(9)
O(1)	Eu(1)	O(7)	73.75(9)	N(3)	Eu(1)	N(1)	61.62(10)
O(1)	Eu(1)	N(1)	63.67(9)	O(5)	Eu(1)	O(2)	71.27(9)
O(1)	Eu(1)	N(3)	125.16(9)	O(5)	Eu(1)	O(3)	138.94(9)
O(2)	Eu(1)	N(1)	120.26(10)	O(5)	Eu(1)	O(6)	141.89(9)
O(2)	Eu(1)	N(3)	138.86(9)	O(5)	Eu(1)	O(7)	132.25(9)
O(3)	Eu(1)	O(2)	69.09(9)	O(5)	Eu(1)	N(1)	66.36(9)
O(3)	Eu(1)	O(6)	70.12(9)	O(5)	Eu(1)	N(3)	73.97(9)
O(3)	Eu(1)	O(7)	72.58(9)	O(6)	Eu(1)	O(2)	118.75(10)
O(3)	Eu(1)	N(1)	127.86(9)	O(6)	Eu(1)	O(7)	70.84(9)
O(3)	Eu(1)	N(3)	146.64(9)	O(6)	Eu(1)	N(1)	120.70(9)
O(4)	Eu(1)	O(1)	137.39(9)	O(6)	Eu(1)	N(3)	78.19(9)
O(4)	Eu(1)	O(2)	69.69(9)	O(7)	Eu(1)	O(2)	132.46(9)
O(4)	Eu(1)	O(3)	103.06(9)	O(7)	Eu(1)	N(1)	66.11(9)
O(4)	Eu(1)	O(5)	72.22(9)	O(7)	Eu(1)	N(3)	87.67(9)

Table S7 Selected least-squares planes data for [Eu(**L2**)(hfac)$_3$] (**2**).

Least-square planes

Least-squares planes description	Abbreviation	Max. deviation/Å	Atom
Pyridine N1, C1, C2, C3, C4, C5	Py	0.0216 (12)	N1
Benzimidazole N3, C12, C13, C14, C15, C16, C17, N4, C11	Bz	0.0148 (11)	N3
Hexafluoroacetylacetonate O4, C25, C26, C27, O5, Eu1	Hfa I	0.0236 (11)	C27
Hexafluoroacetylacetonate O6, C32, C31, C30, O7, Eu1	Hfa II	0.0184 (11)	C30
Hexafluroacetylacetonate O2, C21, C22, C20, O3, Eu1	Hfa III	0.0095 (11)	C22

Interplanar angles (°)

	Bz	Py	Hfa I	Hfa II
Py	10.749 (31)			
Hfa I	80.818 (38)	71.551 (42)		
Hfa II	74.816 (38)	64.793 (41)	10.906 (36)	
Hfa III	102.047 (27)	106.904 (34)	90.154 (41)	100.249 (40)

Table S8 Selected bond distances (Å), bond angles (°) in [Lu(**L2**)(hfac)$_3$] (**5**).

Bond distances (Å)

Atom 1	Atom 2	Distance	Atom 1	Atom 2	Distance
Lu(1)	O(1)	2.2996(18)	Lu(1)	O(6)	2.3924(18)
Lu(1)	O(2)	2.3359(18)	Lu(1)	O(7)	2.3090(18)
Lu(1)	O(3)	2.2937(17)	Lu(1)	N(1)	2.505(2)
Lu(1)	O(4)	2.3661(17)	Lu(1)	N(3)	2.487(2)
Lu(1)	O(5)	2.3703(18)			

Angles (°)

At. 1	At. 2	At. 3	Angle	At. 1	At. 2	At. 3	Angle
O(6)	Lu(1)	N(1)	117.15(7)	O(2)	Lu(1)	O(6)	68.62(6)
O(6)	Lu(1)	N(3)	134.61(7)	O(2)	Lu(1)	N(1)	68.91(6)
O(7)	Lu(1)	O(2)	139.87(6)	O(2)	Lu(1)	N(3)	70.92(6)
O(7)	Lu(1)	O(4)	70.04(6)	O(3)	Lu(1)	O(1)	139.40(6)
O(7)	Lu(1)	O(5)	74.84(6)	O(3)	Lu(1)	O(2)	74.68(6)
O(7)	Lu(1)	O(6)	71.26(7)	O(3)	Lu(1)	O(4)	70.41(6)
O(7)	Lu(1)	N(1)	131.88(7)	O(3)	Lu(1)	O(5)	141.56(6)
O(7)	Lu(1)	N(3)	145.60(7)	O(3)	Lu(1)	O(6)	69.61(6)
N(3)	Lu(1)	N(1)	63.83(7)	O(3)	Lu(1)	O(7)	92.66(7)
O(1)	Lu(1)	O(2)	88.49(6)	O(3)	Lu(1)	N(1)	135.40(7)
O(1)	Lu(1)	O(3)	136.56(6)	O(3)	Lu(1)	N(3)	80.70(7)
O(1)	Lu(1)	O(5)	73.80(6)	O(4)	Lu(1)	O(5)	71.16(6)
O(1)	Lu(1)	O(6)	69.87(6)	O(4)	Lu(1)	O(6)	121.65(6)
O(1)	Lu(1)	O(7)	76.69(7)	O(4)	Lu(1)	N(1)	121.19(6)
O(1)	Lu(1)	N(1)	64.91(6)	O(4)	Lu(1)	N(3)	75.97(6)
O(1)	Lu(1)	N(3)	128.66(6)	O(5)	Lu(1)	O(6)	134.71(6)
O(2)	Lu(1)	O(4)	134.88(6)	O(5)	Lu(1)	N(1)	67.62(6)
O(2)	Lu(1)	O(5)	136.53(6)	O(5)	Lu(1)	N(3)	89.51(6)

Table S9 Selected least-squares planes data for [Lu(**L2**)(hfac)$_3$] (**5**).

Least-square planes

Least-squares planes description	Abbreviation	Max. deviation/Å	Atom
Benzimidazole C11 N3 C12 C13 C14 C15 C16 C17 N4	Bz	0.0155(10)	C17
Pyridine N1 C1 C2 C3 C4 C5	Py	0.0105(12)	N1
Hexafluoroacetylacetonate O3 C42 C41 C40 O8	Hfa I	0.0316(11)	C20
Hexafluoroacetylacetonate O4 C45 C46 C47 O5	Hfa II	0.0134(11)	C25
Hexafluoroacetylacetonate O6 C50 C51 C52 O7	Hfa III	0.0093(11)	C30

Interplanar angles (°)

	Bz	Py	Hfa I	Hfa II
Py	3.71(3)			
Hfa I	67.04(4)	64.96(4)		
Hfa II	68.44(4)	67.21(4)	14.20(3)	
Hfa III	75.98(3)	79.50(3)	80.64(4)	84.19(4)

Table S10 Selected bond distances (Å), bond angles (°) in $[Eu_2(\mathbf{L3})(hfac)_6]$ (**3**).

Bond distances (Å)

Atom 1	Atom 2	Distance	Atom 1	Atom 2	Distance
Eu(1)	O(1)	2.384(5)	Eu(2)	O(2)	2.389(6)
Eu(1)	O(3)	2.384(5)	Eu(2)	O(10)	2.392(5)
Eu(1)	O(4)	2.399(6)	Eu(2)	O(15)	2.393(6)
Eu(1)	O(7)	2.412(5)	Eu(2)	O(11)	2.406(5)
Eu(1)	O(9)	2.433(5)	Eu(2)	O(14)	2.453(5)
Eu(1)	O(5)	2.436(5)	Eu(2)	O(12)	2.461(5)
Eu(1)	O(8)	2.450(6)	Eu(2)	N(7)	2.579(6)
Eu(1)	N(3)	2.581(6)	Eu(2)	N(5)	2.622(6)
Eu(1)	N(1)	2.637(6)	Eu(1)	Eu(2)	12.594(1)
Eu(2)	O(13)	2.381(5)			

Angles (°)

At. 1	At. 2	At. 3	Angle	At. 1	At. 2	At. 3	Angle
O(1)	Eu(1)	O(3)	80.8(2)	O(7)	Eu(1)	O(8)	73.5(2)
O(1)	Eu(1)	O(4)	140.3(2)	O(9)	Eu(1)	O(8)	70.50(17)
O(3)	Eu(1)	O(4)	72.4(2)	O(5)	Eu(1)	O(8)	136.5(2)
O(1)	Eu(1)	O(7)	76.1(2)	O(1)	Eu(1)	N(3)	125.52(18)
O(3)	Eu(1)	O(7)	138.9(2)	O(3)	Eu(1)	N(3)	75.6(2)
O(4)	Eu(1)	O(7)	105.9(2)	O(4)	Eu(1)	N(3)	75.6(2)
O(1)	Eu(1)	O(9)	136.72(19)	O(7)	Eu(1)	N(3)	145.1(2)
O(3)	Eu(1)	O(9)	142.5(2)	O(9)	Eu(1)	N(3)	78.12(18)
O(4)	Eu(1)	O(9)	75.37(19)	O(5)	Eu(1)	N(3)	138.4(2)
O(7)	Eu(1)	O(9)	68.92(19)	O(8)	Eu(1)	N(3)	85.1(2)
O(1)	Eu(1)	O(5)	74.8(2)	O(1)	Eu(1)	N(1)	64.01(18)
O(3)	Eu(1)	O(5)	72.6(2)	O(3)	Eu(1)	N(1)	63.9(2)
O(4)	Eu(1)	O(5)	69.7(2)	O(4)	Eu(1)	N(1)	124.1(2)
O(7)	Eu(1)	O(5)	68.8(2)	O(7)	Eu(1)	N(1)	129.9(2)
O(9)	Eu(1)	O(5)	113.24(19)	O(9)	Eu(1)	N(1)	123.58(18)
O(1)	Eu(1)	O(8)	75.9(2)	O(5)	Eu(1)	N(1)	123.16(19)
O(3)	Eu(1)	O(8)	132.30(18)	O(8)	Eu(1)	N(1)	68.49(18)
O(4)	Eu(1)	O(8)	143.52(19)	N(3)	Eu(1)	N(1)	61.52(18)
O(13)	Eu(2)	O(2)	78.5(2)	O(15)	Eu(2)	O(12)	121.3(2)
O(13)	Eu(2)	O(10)	99.90(18)	O(11)	Eu(2)	O(12)	72.71(18)
O(2)	Eu(2)	O(10)	139.5(2)	O(14)	Eu(2)	O(12)	131.84(18)
O(13)	Eu(2)	O(15)	70.66(18)	O(13)	Eu(2)	N(7)	143.76(19)
O(2)	Eu(2)	O(15)	137.79(19)	O(2)	Eu(2)	N(7)	124.94(19)
O(10)	Eu(2)	O(15)	75.25(18)	O(10)	Eu(2)	N(7)	79.59(18)
O(13)	Eu(2)	O(11)	142.19(18)	O(15)	Eu(2)	N(7)	74.30(19)
O(2)	Eu(2)	O(11)	84.4(2)	O(11)	Eu(2)	N(7)	72.71(19)
O(10)	Eu(2)	O(11)	72.36(17)	O(14)	Eu(2)	N(7)	87.72(17)
O(15)	Eu(2)	O(11)	137.03(18)	O(12)	Eu(2)	N(7)	139.72(18)
O(13)	Eu(2)	O(14)	71.88(17)	O(13)	Eu(2)	N(5)	130.95(18)
O(2)	Eu(2)	O(14)	73.7(2)	O(2)	Eu(2)	N(5)	63.29(18)
O(10)	Eu(2)	O(14)	144.85(19)	O(10)	Eu(2)	N(5)	129.08(17)

O(15)	Eu(2)	O(14)	69.77(18)	O(15)	Eu(2)	N(5)	119.24(19)
O(11)	Eu(2)	O(14)	134.49(17)	O(11)	Eu(2)	N(5)	65.69(17)
O(13)	Eu(2)	O(12)	69.89(19)	O(14)	Eu(2)	N(5)	68.84(19)
O(2)	Eu(2)	O(12)	70.9(2)	O(12)	Eu(2)	N(5)	119.4(2)
O(10)	Eu(2)	O(12)	70.8(2)	N(7)	Eu(2)	N(5)	61.67(19)

Table S11 Selected least-squares planes data for $[Eu_2(\mathbf{L3})(hfac)_6]$ (**3**).

Least-Squares Planes

Least-squares planes description	Abbreviation	Max. deviation /Å	Atom
Benzimidazole 1 C11 N3 C12 C13 C14 C15 C16 C17 N4	Bz1	0.0421 (11)	C14
Pyridine 1 C1 C2 C3 C4 C5 N1	Py1	0.0160 (12)	C3
Benzimidazole 2 C21 C22 C23 N7 C24 N8 C25 C26 C27	Bz2	0.0489 (11)	C21
Pyridine 2 N5 C30 C31 C32 C33 C34	Py2	0.0135 (12)	C32
Hexafluoroacetylacetonate O3 C40 C41 C42 O4	Hfa I	0.0538 (11)	C42
Hexafluoroacetylacetonate O8 C51 C52 C53 O9	Hfa II	0.0225 (11)	C51
Hexafluoroacetylacetonate O5 C45 C46 C47 O7	Hfa III	0.0221 (12)	C46
Hexafluoroacetylacetonate O10 C56 C57 C58 O11	Hfa IV	0.0398 (11)	C58
Hexafluoroacetylacetonate O14 C66 C67 C68 O15	Hfa V	0.0315 (11)	C68
Hexafluoroacetylacetonate O12 C61 C62 C63 O13	Hfa VI	0.0232 (11)	C61

Interplanar angles (°)

	Bz1	Py1	Bz2	Py2	Hfa I	Hfa II	Hfa III	Hfa IV	Hfa V
Bz1									
Py1	18.47(3)								
Bz2	54.25(2)	69.53(3)							
Py2	57.71(3)	74.12(4)	7.30(3)						
Hfa I	74.52(4)	58.74(4)	98.75(3)	106.05(4)					
Hfa II	78.95(4)	62.84(4)	102.84(4)	110.13(4)	4.70(5)				
Hfa III	75.89(3)	71.81(4)	118.85(3)	116.59(4)	99.48(4)	99.29(4)			
Hfa IV	89.89(3)	73.66(4)	109.72(4)	116.88(4)	15.44(4)	10.95(4)	102.37(4)		
Hfa V	82.97(4)	65.32(4)	113.85(4)	121.14(4)	15.29(4)	11.95(4)	89.48(4)	13.44(3)	
Hfa VI	61.03(3)	55.14(4)	109.82(3)	109.58(3)	87.33(4)	88.14(4)	16.86(4)	93.61(4)	80.18(4)

Table S12 Selected bond distances (Å), bond angles (°) in $[Lu_2(\mathbf{L3})(hfac)_6]$ (6).

Bond distances (Å)

Atom 1	Atom 2	Distance	Atom 1	Atom 2	Distance
Lu(1)	O(8)	2.266(4)	Lu(1)	O(7)	2.381(4)
Lu(1)	O(1)	2.284(4)	Lu(1)	O(3)	2.394(4)
Lu(1)	O(5)	2.326(4)	Lu(1)	N(1)	2.474(5)
Lu(1)	O(6)	2.354(4)	Lu(1)	N(3)	2.479(5)
Lu(1)	O(4)	2.375(5)	Lu(1)	Lu(2)	12.533 (1)
Lu(2)	O(10)	2.279(4)	Lu(2)	O(14)	2.388(4)
Lu(2)	O(2)	2.296(4)	Lu(2)	O(13)	2.395(4)
Lu(2)	O(11)	2.339(4)	Lu(2)	N(5)	2.496(5)
Lu(2)	O(12)	2.360(5)	Lu(2)	N(7)	2.507(5)
Lu(2)	O(9)	2.379(4)			

Angles (°)

At. 1	At. 2	At. 3	Angle	At. 1	At. 2	At. 3	Angle
O(8)	Lu(1)	O(1)	139.66(17)	O(6)	Lu(1)	O(3)	134.53(15)
O(8)	Lu(1)	O(5)	100.86(17)	O(4)	Lu(1)	O(3)	69.23(16)
O(1)	Lu(1)	O(5)	76.42(17)	O(7)	Lu(1)	O(3)	138.70 (16)
O(8)	Lu(1)	O(6)	140.86(16)	O(8)	Lu(1)	N(1)	128.34(17)
O(1)	Lu(1)	O(6)	77.73(15)	O(1)	Lu(1)	N(1)	65.27(17)
O(5)	Lu(1)	O(6)	72.92(15)	O(5)	Lu(1)	N(1)	130.76(16)
O(8)	Lu(1)	O(4)	70.02(17)	O(6)	Lu(1)	N(1)	69.76(14)
O(1)	Lu(1)	O(4)	70.77(16)	O(4)	Lu(1)	N(1)	117.89(17)
O(5)	Lu(1)	O(4)	73.30(16)	O(7)	Lu(1)	N(1)	123.82(16)
O(6)	Lu(1)	O(4)	138.06(16)	O(3)	Lu(1)	N(1)	64.77(15)
O(8)	Lu(1)	O(7)	72.25(16)	O(8)	Lu(1)	N(3)	76.25(17)
O(1)	Lu(1)	O(7)	137.18(15)	O(1)	Lu(1)	N(3)	129.64(16)
O(5)	Lu(1)	O(7)	68.12(16)	O(5)	Lu(1)	N(3)	142.45(16)
O(6)	Lu(1)	O(7)	69.65(13)	O(6)	Lu(1)	N(3)	85.94(15)
O(4)	Lu(1)	O(7)	118.28(16)	O(4)	Lu(1)	N(3)	135.67(16)
O(8)	Lu(1)	O(3)	73.60(17)	O(7)	Lu(1)	N(3)	75.60(15)
O(1)	Lu(1)	O(3)	84.44(17)	O(3)	Lu(1)	N(3)	74.31(16)
O(5)	Lu(1)	O(3)	141.71(17)	N(1)	Lu(1)	N(3)	64.38(16)
O(10)	Lu(2)	O(2)	141.33(16)	O(12)	Lu(2)	O(13)	119.47(16)
O(10)	Lu(2)	O(11)	100.34(15)	O(9)	Lu(2)	O(13)	139.68(15)
O(2)	Lu(2)	O(11)	75.26(16)	O(14)	Lu(2)	O(13)	69.17(14)
O(10)	Lu(2)	O(12)	70.32(16)	O(10)	Lu(2)	N(5)	128.13(15)
O(2)	Lu(2)	O(12)	71.73(17)	O(2)	Lu(2)	N(5)	65.02(16)
O(11)	Lu(2)	O(12)	73.12(16)	O(11)	Lu(2)	N(5)	131.41(15)
O(10)	Lu(2)	O(9)	73.81(15)	O(12)	Lu(2)	N(5)	116.30(16)
O(2)	Lu(2)	O(9)	85.19(16)	O(9)	Lu(2)	N(5)	64.52(15)
O(11)	Lu(2)	O(9)	139.86(16)	O(14)	Lu(2)	N(5)	70.67(14)
O(12)	Lu(2)	O(9)	67.50(16)	N(13)	Lu(2)	N(5)	124.23(15)
O(10)	Lu(2)	O(14)	140.84(14)	O(10)	Lu(2)	N(7)	76.63(15)
O(2)	Lu(2)	O(14)	75.78(16)	O(2)	Lu(2)	N(7)	129.02(15)

O(11)	Lu(2)	O(14)	73.45(15)	O(11)	Lu(2)	N(7)	143.79(15)
O(12)	Lu(2)	O(14)	138.02(16)	O(12)	Lu(2)	N(7)	135.12(16)
O(9)	Lu(2)	O(14)	135.20(14)	O(9)	Lu(2)	N(7)	74.80(16)
O(10)	Lu(2)	O(13)	72.61(15)	O(14)	Lu(2)	N(7)	86.32(16)
O(2)	Lu(2)	O(13)	135.10(16)	O(13)	Lu(2)	N(7)	76.29(15)
O(11)	Lu(2)	O(13)	68.59(15)	N(5)	Lu(2)	N(7)	64.03(15)

Table S13 Selected least-squares planes data for for $[Lu_2(\mathbf{L3})(hfac)_6]$ (**6**).

Least-Squares Planes

Least-squares planes description	Abbreviation	Max. deviation /Å	Atom
Benzimidazole 1 C11 N3 C12 C13 C14 C15 C16 C17 N4	Bz1	0.0511 (10)	C12
Pyridine 1 C1 C2 C3 C4 C5 N1	Py1	0.0110 (12)	N1
Benzimidazole 2 C21 C22 C23 N7 C24 N8 C25 C26 C27	Bz2	0.0435 (11)	C21
Pyridine 2 C30 C31 C32 C33 C34 N5	Py2	0.0097 (12)	C34
Hexafluoroacetylacetonate O3 C42 C41 C40 O8	Hfa I	0.0275 (11)	C40
Hexafluoroacetylacetonate O6 C50 C51 C52 O7	Hfa II	0.0190 (11)	C50
Hexafluoroacetylacetonate O4 C45 C46 C47 O5	Hfa III	0.0071 (12)	C46
Hexafluoroacetylacetonate O9 C55 C56 C57 O10	Hfa IV	0.0189 (11)	C57
Hexafluoroacetylacetonate O13 C65 C66 C67 O14	Hfa V	0.0212 (11)	C67
Hexafluoroacetylacetonate O11 C62 C61 C60 O12	Hfa VI	0.0084 (12)	C61

Interplanar angles (°)

	Bz1	Py1	Bz2	Py2	Hfa I	Hfa II	Hfa III	Hfa IV	Hfa V
Py1	4.76(3)								
Bz2	60.67(3)	59.10(3)							
Py2	72.86(3)	71.94(3)	14.52(3)						
Hfa I	118.43(4)	122.18(4)	90.68(3)	77.28(3)					
Hfa II	107.77(4)	111.14(4)	79.37(4)	66.63(4)	12.42(5)				
Hfa III	101.85(3)	97.54(3)	59.06(3)	59.44(4)	107.14(4)	105.02(4)			
Hfa IV	103.57(3)	106.69(4)	73.56(4)	60.99(4)	18.16(4)	5.89(5)	102.27(5)		
Hfa V	109.96(4)	113.02(4)	76.83(4)	63.55(4)	13.86(4)	5.31(3)	99.75(4)	6.44(4)	
Hfa VI	115.16(3)	110.80(4)	69.80(3)	67.52(4)	100.33(4)	100.91(4)	13.40(3)	99.43(4)	95.63(4)

Table S14 Selected bond distances (Å), bond angles (°) in $[Eu_3(\mathbf{L4})(hfac)_9]$ (**4**).

Bond distances (Å)

Atom 1	Atom 2	Distance	Atom 1	Atom 2	Distance
Eu(1)	O(5H)	2.372(4)	Eu(2)	O(11H)	2.469(4)
Eu(1)	O(6H)	2.402(4)	Eu(2)	N(4)	2.567(4)
Eu(1)	O(3H)	2.402(4)	Eu(2)	N(6)	2.593(4)
Eu(1)	O(1H)	2.410(4)	Eu(3)	O(13H)	2.399(4)
Eu(1)	O(2H)	2.471(4)	Eu(3)	O(15H)	2.409(4)
Eu(1)	O(4H)	2.482(4)	Eu(3)	O(2)	2.422(4)
Eu(1)	N(2)	2.525(4)	Eu(3)	O(16H)	2.425(4)
Eu(1)	N(8)	2.547(4)	Eu(3)	O(14H)	2.425(4)
Eu(1)	N(1)	2.643(4)	Eu(3)	O(18H)	2.435(4)
Eu(2)	O(7H)	2.387(4)	Eu(3)	O(17H)	2.435(4)
Eu(2)	O(10H)	2.396(4)	Eu(3)	N(10)	2.598(4)
Eu(2)	O(12H)	2.409(4)	Eu(3)	N(12)	2.611(5)
Eu(2)	O(1)	2.412(4)	Eu(3)	Eu(1)	12.806(1)
Eu(2)	O(9H)	2.434(4)	Eu(1)	Eu(2)	9.593(1)
Eu(2)	O(8H)	2.446(3)	Eu(2)	Eu(3)	19.051(1)

Angles (°)

At. 1	At. 2	At. 3	Angle	At. 1	At. 2	At. 3	Angle
O(5H)	Eu(1)	O(6H)	75.31(15)	O(1)	Eu(2)	O(11H)	73.81(14)
O(5H)	Eu(1)	O(3H)	81.65(15)	O(9H)	Eu(2)	O(11H)	132.18(13)
O(6H)	Eu(1)	O(3H)	135.71(15)	O(8H)	Eu(2)	O(11H)	136.49(13)
O(5H)	Eu(1)	O(1H)	139.94(15)	O(7H)	Eu(2)	N(4)	80.73(13)
O(6H)	Eu(1)	O(1H)	80.39(14)	O(10H)	Eu(2)	N(4)	143.49(13)
O(3H)	Eu(1)	O(1H)	136.22(13)	O(12H)	Eu(2)	N(4)	76.12(13)
O(5H)	Eu(1)	O(2H)	72.50(14)	O(1)	Eu(2)	N(4)	125.18(13)
O(6H)	Eu(1)	O(2H)	67.21(14)	O(9H)	Eu(2)	N(4)	141.15(13)
O(3H)	Eu(1)	O(2H)	139.06(13)	O(8H)	Eu(2)	N(4)	76.63(12)
O(1H)	Eu(1)	O(2H)	68.86(12)	O(11H)	Eu(2)	N(4)	85.96(13)
O(5H)	Eu(1)	O(4H)	71.38(14)	O(7H)	Eu(2)	N(6)	130.40(13)
O(6H)	Eu(1)	O(4H)	67.92(15)	O(10H)	Eu(2)	N(6)	129.02(15)
O(3H)	Eu(1)	O(4H)	69.05(14)	O(12H)	Eu(2)	N(6)	121.27(13)
O(1H)	Eu(1)	O(4H)	126.93(14)	O(1H)	Eu(2)	N(6)	63.38(12)
O(2H)	Eu(1)	O(4H)	127.70(13)	O(9H)	Eu(2)	N(6)	119.53(13)
O(5H)	Eu(1)	N(2)	82.67(14)	O(8H)	Eu(2)	N(6)	68.61(12)
O(6H)	Eu(1)	N(2)	139.08(14)	O(11H)	Eu(2)	N(6)	68.01(13)
O(3H)	Eu(1)	N(2)	72.14(14)	N(4)	Eu(2)	N(6)	61.81(13)
O(1H)	Eu(1)	N(2)	96.04(14)	O(13H)	Eu(3)	O(15H)	72.05(13)
O(2H)	Eu(1)	N(2)	73.49(13)	O(13H)	Eu(3)	O(2)	140.61(14)
O(4H)	Eu(1)	N(2)	135.67(14)	O(15H)	Eu(3)	O(2)	139.76(13)
O(5H)	Eu(1)	N(8)	141.41(14)	O(13H)	Eu(3)	O(16H)	137.39(13)
O(6H)	Eu(1)	N(8)	89.66(13)	O(15H)	Eu(3)	O(16H)	71.76(13)
O(3H)	Eu(1)	N(8)	85.35(14)	O(2)	Eu(3)	O(16H)	81.96(13)
O(1H)	Eu(1)	N(8)	68.33(13)	O(13H)	Eu(3)	O(14H)	71.09(14)
O(2H)	Eu(1)	N(8)	133.95(13)	O(15H)	Eu(3)	O(14H)	141.85(14)
O(4H)	Eu(1)	N(8)	70.03(13)	O(2)	Eu(3)	O(14H)	77.74(14)
N(2)	Eu(1)	N(8)	127.14(13)	O(16H)	Eu(3)	O(14H)	134.95(14)
O(5H)	Eu(1)	N(1)	138.18(14)	O(13H)	Eu(3)	O(18H)	112.49(15)
O(6H)	Eu(1)	N(1)	146.51(13)	O(15H)	Eu(3)	O(18H)	69.69(13)
O(3H)	Eu(1)	N(1)	65.56(13)	O(2)	Eu(3)	O(18H)	74.25(13)
O(1H)	Eu(1)	N(1)	71.42(12)	O(16H)	Eu(3)	O(18H)	74.38(14)

O(2H)	Eu(1)	N(1)	116.32(13)	O(14H)	Eu(3)	O(18H)	135.08(14)
O(4H)	Eu(1)	N(1)	115.88(13)	O(13H)	Eu(3)	O(17H)	69.25(16)
N(2)	Eu(1)	N(1)	63.57(13)	O(15H)	Eu(3)	O(17H)	104.08(15)
N(8)	Eu(1)	N(1)	63.58(13)	O(2)	Eu(3)	O(17H)	78.48(15)
O(7H)	Eu(2)	O(10H)	100.52(15)	O(16H)	Eu(3)	O(17H)	142.00(14)
O(7H)	Eu(2)	O(12H)	74.27(14)	O(14H)	Eu(3)	O(17H)	71.40(15)
O(10H)	Eu(2)	O(12H)	69.36(14)	O(18H)	Eu(3)	O(17H)	69.11(15)
O(7H)	Eu(2)	O(1)	140.02(13)	O(13H)	Eu(3)	N(10)	75.92(15)
O(10H)	Eu(2)	O(1)	76.52(14)	O(15H)	Eu(3)	N(10)	75.90(13)
O(12H)	Eu(2)	O(1)	136.27(14)	O(2)	Eu(3)	N(10)	125.77(14)
O(7H)	Eu(2)	O(9H)	71.04(14)	O(16H)	Eu(3)	N(10)	74.11(14)
O(10H)	Eu(2)	O(9H)	69.73(14)	O(14H)	Eu(3)	N(10)	85.97(14)
O(12H)	Eu(2)	O(9H)	118.99(14)	O(18H)	Eu(3)	N(10)	138.95(13)
O(1)	Eu(2)	O(9H)	70.67(13)	O(17H)	Eu(3)	N(10)	142.97(15)
O(7H)	Eu(2)	O(8H)	72.14(13)	O(13H)	Eu(3)	N(12)	121.06(15)
O(10H)	Eu(2)	O(8H)	138.93(13)	O(15H)	Eu(3)	N(12)	127.44(14)
O(12H)	Eu(2)	O(8H)	139.44(14)	O(2)	Eu(3)	N(12)	64.20(13)
O(1)	Eu(2)	O(8H)	84.22(13)	O(16H)	Eu(3)	N(12)	67.91(13)
O(9H)	Eu(2)	O(8H)	69.74(13)	O(14H)	Eu(3)	N(12)	67.06(14)
O(7H)	Eu(2)	O(11H)	144.02(14)	O(18H)	Eu(3)	N(12)	126.43(14)
O(10H)	Eu(2)	O(11H)	71.66(14)	O(17H)	Eu(3)	N(12)	128.45(15)
O(12H)	Eu(2)	O(11H)	70.11(15)	O(10)	Eu(3)	N(12)	61.79(14)

Table S15 Selected least-squares planes data for $[Eu_3(\mathbf{L4})(hfac)_9]$ (**4**).

Least-Squares Planes

Least-squares planes description	Abbreviation	Max. deviation /Å	Atom
Benzimidazole 1 C6 N2 C7 C8 C9 C10 C11 C12 N3	Bz1	0.0283 (11)	C6
Pyridine 1 C1 C2 C3 C4 C5 N1	Py1	0.0079 (12)	C5
Benzimidazole 2 C31 N8 C32 C33 C34 C35 C36 C37 N9	Bz2	0.0137 (11)	C31
Pyridine 2 C21 C22 C23 C24 C25 N6	Py2	0.0262 (12)	N6
Benzimidazole 3 N4 C16 C15 C14 C19 C18 C17 N5	Bz3	0.0279 (12)	N4
Benzimidazole 4 C39 C40 C41 N10 C45 N11 C42 C43 C44	Bz4	0.0124 (11)	N10
Pyridine 3 N12 C46 C47 C48 C49 C50	Py3	0.0403 (12)	N12
Hexafluoroacetylacetonate O1H C1H C2H C3H O2H	Hfa I	0.0341 (11)	C1H
Hexafluoroacetylacetonate O3H C6H C7H C8H O4H	Hfa II	0.0203 (11)	C8H
Hexafluoroacetylacetonate O5H C11H C12H C13H O6H	Hfa III	0.0004 (11)	C11H
Hexafluoroacetylacetonate O7H C16H C17H C18H O8H	Hfa IV	0.0118 (11)	C18H
Hexafluoroacetylacetonate O11H C26H C27H C28H O12H	Hfa V	0.0006 (11)	C28H
Hexafluoroacetylacetonate O9H C21H C22H C23H O10H	Hfa VI	0.0258 (11)	C21H
Hexafluoroacetylacetonate O16H C36H C37H C38H O15H	Hfa VII	0.0385 (11)	C38H
Hexafluoroacetylacetonate O13H C31H C32H C33H O14H	Hfa VIII	0.0210 (11)	C33H
Hexafluoroacetylacetonate O17H C41H C42H C43H O18H	Hfa IX	0.0097 (11)	C43H

Interplanar angles (°)

	Bz1	Py1	Bz2	Py2	Bz3	Py3	Bz4
Py1	24.33 (3)						
Bz2	155.14 (2)	147.28 (3)					
Py2	72.72 (3)	62.68 (3)	86.24 (3)				
Bz3	82.51 (2)	77.73 (3)	73.86 (2)	17.87 (3)			
Py3	58.89 (3)	37.35 (3)	110.80 (3)	37.24 (3)	55.10 (3)		
Bz4	82.34 (3)	61.12 (3)	87.66 (3)	34.26 (3)	48.61 (2)	23.81 (3)	
Hfa I	100.66 (4)	119.92 (4)	64.25 (4)	86.82 (3)	69.99 (3)	122.30 (3)	117.81 (3)
Hfa II	66.36 (4)	55.10 (4)	93.46 (4)	7.70 (4)	25.04 (4)	30.59 (4)	32.14 (3)
Hfa III	136.09 (3)	136.81 (4)	19.80 (3)	74.47 (4)	59.12 (3)	106.53 (4)	86.69 (4)
Hfa IV	124.17 (3)	146.73 (3)	49.93 (3)	108.28 (4)	90.42 (4)	145.48 (4)	130.48 (4)
Hfa V	62.09 (3)	37.85 (4)	118.86 (3)	60.78 (4)	78.47 (4)	23.97 (4)	36.24 (3)
Hfa VI	142.84 (3)	121.09 (4)	32.73 (4)	74.43 (3)	71.00 (3)	84.34 (4)	60.64 (4)
Hfa VII	19.26 (3)	28.40 (4)	136.18 (3)	54.86 (4)	63.34 (3)	50.59 (4)	71.50 (4)
Hfa VIII	18.35 (3)	42.16 (4)	144.15 (3)	77.01 (4)	81.52 (4)	73.36 (4)	95.33 (4)
Hfa IX	89.11 (4)	103.25 (4)	69.83 (4)	65.73 (3)	49.75 (3)	100.62 (3)	98.34 (3)

	Hfa I	Hfa II	Hfa III	Hfa IV	Hfa V	Hfa VI	Hfa VII	Hfa VIII
Hfa II	92.34 (3)							
Hfa III	49.10 (4)	82.15 (4)						
Hfa IV	28.42 (4)	115.20 (4)	44.45 (5)					
Hfa V	146.04 (4)	54.47 (4)	122.39 (4)	166.70 (4)				
Hfa VI	94.36 (5)	79.33 (4)	45.40 (4)	82.58 (4)	86.85 (4)			
Hfa VII	91.53 (4)	49.29 (4)	118.10 (3)	118.97 (4)	62.45 (4)	128.49 (4)		
Hfa VIII	83.16 (4)	72.37 (5)	124.53 (3)	105.82 (3)	80.10 (4)	151.43 (4)	24.07 (5)	
Hfa IX	21.67 (3)	70.86 (3)	50.64 (4)	48.60 (4)	124.40 (4)	92.93 (4)	75.51 (4)	74.40 (4)

Table S16 Bond Distances ($\delta_{i,j}$), Bond Valences ($v_{\mathrm{Ln,j}}$)[a] and Total Atom Valence (V_{Ln})[b] in the Crystal Structure of [Eu(**L2**)(hfac)$_3$] (**2**).

Atom[c]	Donor type	$\delta_{\mathrm{Eu},j}$ / Å	$v_{\mathrm{Eu},j}$	
N3	bzim	2.566	0.335	Average N-heterocyclic
N1	py	2.612	0.296	0.32 (3)
O1	amide	2.396	0.380	
O2	hfac	2.450	0.328	
O3	hfac	2.417	0.359	
O4	hfac	2.394	0.382	
O5	hfac	2.397	0.379	
O6	hfac	2.421	0.355	Average O-hfac
O7	hfac	2.445	0.333	0.36 (2)
		V_{Eu}	3.147	

[a] $v_{\mathrm{Ln},j} = e^{\left[\left(R_{\mathrm{Ln},j} - d_{\mathrm{Ln},j}\right)/b\right]}$, whereby $\delta_{\mathrm{Ln},j}$ is the Ln-donor atom j distance. The valence bond parameters $R_{\mathrm{Ln,N}}$ and $R_{\mathrm{Ln,O}}$ are taken from ref 29e,f and b = 0.37 Å. [b] $V_{\mathrm{Ln}} = \sum_j v_{\mathrm{Ln},j}$. [c] Numbering taken from Fig S1a.

Table S17 Bond Distances ($\delta_{i,j}$), Bond Valences ($v_{\mathrm{Ln,j}}$)[a] and Total Atom Valence (V_{Ln})[b] in the Crystal Structure of [Lu(**L2**)(hfac)$_3$] (**5**).

Atom[c]	Donor type	$\delta_{\mathrm{Lu},j}$ / Å	$v_{\mathrm{Lu},j}$	
N3	bzim	2.487	0.304	Average N-heterocyclic
N1	py	2.505	0.289	0.30 (1)
O1	amide	2.300	0.386	
O2	hfac	2.336	0.350	
O3	hfac	2.294	0.392	
O4	hfac	2.366	0.322	
O5	hfac	2.370	0.319	
O6	hfac	2.392	0.300	Average O-hfac
O7	hfac	2.309	0.376	0.34 (4)
		V_{Lu}	3.036	

[a] $v_{\mathrm{Ln},j} = e^{\left[\left(R_{\mathrm{Ln},j} - d_{\mathrm{Ln},j}\right)/b\right]}$, whereby $\delta_{\mathrm{Ln},j}$ is the Ln-donor atom j distance. The valence bond parameters $R_{\mathrm{Ln,N}}$ and $R_{\mathrm{Ln,O}}$ are taken from ref 29e,f and b = 0.37 Å. [b] $V_{\mathrm{Ln}} = \sum_j v_{\mathrm{Ln},j}$. [c] Numbering taken from Fig S1b.

Table S18 Bond Distances ($\delta_{i,j}$), Bond Valences ($v_{\mathrm{Ln,j}}$)[a] and Total Atom Valence (V_{Ln})[b] in the Crystal Structure of [Eu_2(**L3**)(hfac)$_6$] (**3**).

Atom[c]	Donor type	$\delta_{\mathrm{Eu},j}$ / Å	$v_{\mathrm{Eu},j}$	
N3	bzim	2.581	0.321	Average N-heterocyclic
N1	py	2.637	0.276	0.30 (3)
O1	amide	2.384	0.393	
O3	hfac	2.384	0.393	
O4	hfac	2.399	0.377	
O8	hfac	2.450	0.328	
O9	hfac	2.433	0.344	
O5	hfac	2.436	0.341	Average O-hfac
O7	hfa	2.412	0.364	0.36 (2)
		V_{Eu1}	3.137	
N7	bzim	2.579	0.323	Average N-heterocyclic
N5	py	2.622	0.288	0.31 (3)
O2	amide	2.389	0.387	
O10	hfac	2.392	0.384	
O11	hfac	2.406	0.370	
O14	hfac	2.453	0.326	
O15	hfac	2.393	0.383	
O12	hfac	2.461	0.319	Average O-hfac
O13	hfac	2.381	0.396	0.36 (3)
		V_{Eu2}	3.175	

[a] $v_{\mathrm{Ln},j} = e^{\left[\left(R_{\mathrm{Ln},j} - d_{\mathrm{Ln},j}\right)/b\right]}$, whereby $\delta_{\mathrm{Ln},j}$ is the Ln-donor atom j distance. The valence bond parameters $R_{\mathrm{Ln,N}}$ and $R_{\mathrm{Ln,O}}$ are taken from ref 29e,f and b = 0.37 Å. [b] $V_{\mathrm{Ln}} = \sum_j v_{\mathrm{Ln},j}$. [c] Numbering taken from Fig S2a.

Table S19 Bond Distances ($\delta_{i,j}$), Bond Valences ($v_{\mathrm{Ln,j}}$)[a] and Total Atom Valence (V_{Ln})[b] in the Crystal Structure of [Lu_2(**L3**)(hfac)$_6$] (**6**).

Atom[c]	Donor type	$\delta_{\mathrm{Lu},j}$ / Å	$v_{\mathrm{Lu},j}$	
N3	bzim	2.479	0.310	Average N-heterocyclic
N1	py	2.474	0.315	0.312 (3)
O1	amide	2.284	0.402	
O3	hfac	2.394	0.299	
O8	hfac	2.266	0.422	
O4	hfac	2.375	0.315	
O5	hfac	2.326	0.359	
O6	hfac	2.354	0.333	Average O-hfac
O7	hfac	2.381	0.309	0.34 (5)
		V_{Lu1}	3.064	
N7	bzim	2.507	0.288	Average N-heterocyclic
N5	py	2.496	0.296	0.29 (1)
O2	amide	2.296	0.389	
O11	hfac	2.339	0.347	
O12	hfac	2.360	0.328	
O9	hfac	2.379	0.311	
O10	hfac	2.279	0.408	
O13	hfac	2.395	0.298	Average O-hfac
O14	hfac	2.388	0.304	0.33 (4)
		V_{Lu2}	2.968	

[a] $v_{\mathrm{Ln},j} = e^{\left[\left(R_{\mathrm{Ln},j} - d_{\mathrm{Ln},j}\right)/b\right]}$, whereby $\delta_{\mathrm{Ln},j}$ is the Ln-donor atom j distance. The valence bond parameters $R_{\mathrm{Ln,N}}$ and $R_{\mathrm{Ln,O}}$ are taken from ref 29e,f and b = 0.37 Å. [b] $V_{\mathrm{Ln}} = \sum_j v_{\mathrm{Ln},j}$. [c] Numbering taken from Fig S2b.

Table S20 Bond Distances ($\delta_{i,j}$), Bond Valences ($v_{\mathrm{Ln,j}}$)[a] and Total Atom Valence (V_{Ln})[b] in the Crystal Structure of [Eu_3(**L4**)(hfac)$_9$] (**4**).

Atom[c]	Donor type	$\delta_{\mathrm{Eu},j}$ / Å	$v_{\mathrm{Eu},j}$	
N2	bzim	2.525	0.374	
N1	py	2.643	0.272	Average N-heterocyclic
N8	bzim	2.547	0.352	0.33 (5)
O1H	hfac	2410	0.366	
O2H	hfac	2.471	0.310	
O3H	hfac	2.402	0.374	
O4H	hfac	2.482	0.301	
O5H	hfac	2.372	0.405	Average O-hfac
O6H	hfac	2.402	0.374	0.36 (4)
		V_{Eu1}	3.129	
N4	bzim	2.567	0.334	Average N-heterocyclic
N6	py	2.593	0.311	0.32 (2)
O1	amide	2.412	0.364	
O7H	hfac	2.387	0.389	
O8H	hfac	2.446	0.332	
O9H	hfac	2.434	0.343	
O10H	hfac	2.396	0.380	
O11H	hfac	2.469	0.312	Average O-hfac
O12H	hfac	2.409	0.367	0.35 (3)
		V_{Eu2}	3.132	
N10	bzim	2.598	0.307	Average N-heterocyclic
N12	py	2.611	0.296	0.30 (1)
O2	amide	2.422	0.354	
O13H	hfac	2.399	0.377	
O14H	hfac	2.425	0.351	
O15H	hfac	2.409	0.367	
O16H	hfac	2.425	0.351	
O17H	hfac	2.435	0.342	Average O-hfac
O18H	hfac	2.435	0.342	0.36 (1)
		V_{Eu3}	3.088	

[a] $v_{\mathrm{Ln},j} = e^{\left[\left(R_{\mathrm{Ln},j} - d_{\mathrm{Ln},j}\right)/b\right]}$, whereby $\delta_{\mathrm{Ln},j}$ is the Ln-donor atom j distance. The valence bond parameters $R_{\mathrm{Ln,N}}$ and $R_{\mathrm{Ln,O}}$ are taken from ref 29e,f and b = 0.37 Å. [b] $V_{\mathrm{Ln}} = \sum_j v_{\mathrm{Ln},j}$. [c] Numbering taken from Fig S3.

Table S21 Helicity indexes *H* of the five-atoms crooked line in the molecular structures of $[Eu_2(\mathbf{L3})(hfac)_6]$ (**3**), $[Lu_2(\mathbf{L3})(hfac)_6]$ (**6**) and $[Eu_3(\mathbf{L4})(hfac)_9]$ (**4**) whree *L* is the end to end distance of the helix, *A* is the area of the subtended figure in the projection plane and *D* is the total length of the crooked line.[30]

Compound	*L* /Å	*A* /Å^2	*D* /Å	*H*
$[Eu_2(\mathbf{L3})(hfac)_6]$	4.32	0.747	5.87	0.52
$[Lu_2(\mathbf{L3})(hfac)_6]$	4.06	0.842	5.78	0.58
$[Eu_3(\mathbf{L4})(hfac)_9]$	3.64	1.290	5.86	0.71
	4.32	1.195	5.87	0.83

Table S22 Summary of crystal data, intensity measurements and structure refinements for $[La(\mathbf{L2})_2(hfac)_2]_2[La_2(hfac)_4(O_2CCF_3)_4]\cdot 2CH_3CN$ (**7**).

	7
Empirical formula	$C_{48}H_{46}F_{12}N_8O_6La$, $0.5(C_{28}H_4F_{36}La_2O_{16})$, $2CH_3CN$
Formula weight	2059.01
Temperature	190 (2) K
Wavelength	1.54184 Å
Crystal System, Space group	triclinic, *P*-1
Unit cell dimensions	a = 11.6721 (2) Å
	b = 15.7298 (4) Å
	c = 22.3967 (5) Å
	α = 78.307 (2)°
	β = 87.1599 (10)°
	γ = 89.3088 (18)°
Volume in Å^3	4018.90 (16)
Z, Calculated density	2, 1.701 Mg/m^3
Absorption coefficient	9.331 mm^{-1}
F(000)	2032
Theta range for data collection	2.87 to 73.48°
Limiting indices	-14<=h<=11,
	-18<=k<=19,
	-27<=l<=27
Reflections collected / unique	28390 / 15744
	[R(int) = 0.05]
Completeness to theta	66.97°/ 99.9 %
Data / restraints / parameters	15744 / 3 / 1091
Goodness-of-fit on F^2	1.051
Final R indices [I>2σ(I)]	R_1 = 0.0522,
	ωR_2 = 0.1400
R indices (all data)	R_1 = 0.0554,
	ωR_2 = 0.1449
Largest diff. peak and hole	1.541 and -1.428 e.Å^{-3}

Table S23 Selected bond distances (Å), bond angles (°) in $[La(\mathbf{L2})_2(hfac)_2]_2[La_2(hfac)_4(O_2CCF_3)_4]$ (**7**).

Bond distances (Å)			Bond distances (Å)		
Atom 1	Atom 2	Distance	Atom 1	Atom 2	Distance
La(1)	N(1A)	2.769(3)	La(1)	O(4H)	2.537(3)
La(1)	N(1B)	2.788(3)	La(2)	O(1C)	2.494(3)
La(1)	N(3A)	2.728(3)	La(2)	O(2C)	2.497(3)
La(1)	N(3B)	2.757(3)	La(2)	O(3C)	2.493(3)
La(1)	O(1A)	2.549(3)	La(2)	O(4C)	2.507(3)
La(1)	O(1B)	2.507(3)	La(2)	O(5C)	2.495(3)
La(1)	O(1H)	2.543(3)	La(2)	O(6C)	2.510(3)
La(1)	O(2H)	2.550(3)	La(2)	O(7C)	2.460(3)
La(1)	O(3H)	2.571(3)	La(2)	O(8C)	2.543(3)

Angles				Angles			
At. 1	At. 2	At. 3	Angle	At. 1	At. 2	At. 3	Angle
O(1B)	La(1)	O(4H)	136.14(10)	O(4H)	La(1)	N(1B)	115.43(10)
O(1B)	La(1)	O(1H)	68.72(11)	O(1H)	La(1)	N(1B)	114.09(10)
O(4H)	La(1)	O(1H)	130.26(10)	O(1A)	La(1)	N(1B)	123.87(10)
O(1B)	La(1)	O(1A)	72.71(10)	O(2H)	La(1)	N(1B)	64.46(10)
O(4H)	La(1)	O(1A)	78.26(9)	O(3H)	La(1)	N(1B)	69.37(10)
O(1H)	La(1)	O(1A)	70.89(10)	N(3A)	La(1)	N(1B)	117.46(10)
O(1B)	La(1)	O(2H)	78.78(10)	N(3B)	La(1)	N(1B)	58.08(10)
O(4H)	La(1)	O(2H)	142.50(9)	N(1A)	La(1)	N(1B)	175.80(10)
O(1H)	La(1)	O(2H)	67.01(10)	O(7C)	La(2)	O(3C)	145.76(12)
O(1A)	La(1)	O(2H)	135.36(10)	O(7C)	La(2)	O(1C)	139.34(12)
O(1B)	La(1)	O(3H)	72.09(11)	O(3C)	La(2)	O(1C)	72.58(12)
O(4H)	La(1)	O(3H)	66.84(10)	O(7C)	La(2)	O(5C)	73.29(12)
O(1H)	La(1)	O(3H)	129.60(10)	O(3C)	La(2)	O(5C)	78.70(12)
O(1A)	La(1)	O(3H)	68.08(10)	O(1C)	La(2)	O(5C)	146.41(11)
O(2H)	La(1)	O(3H)	133.16(10)	O(7C)	La(2)	O(2C)	79.48(12)
O(1B)	La(1)	N(3A)	146.98(10)	O(3C)	La(2)	O(2C)	112.88(12)
O(4H)	La(1)	N(3A)	76.32(9)	O(1C)	La(2)	O(2C)	68.49(11)
O(1H)	La(1)	N(3A)	85.34(10)	O(5C)	La(2)	O(2C)	141.09(12)
O(1A)	La(1)	N(3A)	118.68(10)	O(7C)	La(2)	O(4C)	85.60(13)
O(2H)	La(1)	N(3A)	72.26(10)	O(3C)	La(2)	O(4C)	68.32(12)
O(3H)	La(1)	N(3A)	140.45(10)	O(1C)	La(2)	O(4C)	108.76(12)
O(1B)	La(1)	N(3B)	118.40(10)	O(5C)	La(2)	O(4C)	75.27(12)
O(4H)	La(1)	N(3B)	71.58(10)	O(2C)	La(2)	O(4C)	75.43(11)
O(1H)	La(1)	N(3B)	143.98(10)	O(7C)	La(2)	O(6C)#1	74.07(12)
O(1A)	La(1)	N(3B)	144.62(10)	O(3C)	La(2)	O(6C)#1	139.39(12)
O(2H)	La(1)	N(3B)	79.47(10)	O(1C)	La(2)	O(6C)#1	72.97(12)
O(3H)	La(1)	N(3B)	83.10(10)	O(5C)	La(2)	O(6C)#1	123.54(10)
N(3A)	La(1)	N(3B)	71.77(10)	O(2C)	La(2)	O(6C)#1	72.69(11)
O(1B)	La(1)	N(1A)	123.08(10)	O(4C)	La(2)	O(6C)#1	144.67(12)
O(4H)	La(1)	N(1A)	63.98(10)	O(7C)	La(2)	O(8C)#1	117.79(13)
O(1H)	La(1)	N(1A)	66.98(10)	O(3C)	La(2)	O(8C)#1	75.28(12)

O(1A)	La(1)	N(1A)	60.30(10)	O(1C)	La(2)	O(8C)#1	76.06(12)
O(2H)	La(1)	N(1A)	113.23(10)	O(5C)	La(2)	O(8C)#1	80.14(12)
O(3H)	La(1)	N(1A)	113.33(10)	O(2C)	La(2)	O(8C)#1	138.06(12)
N(3A)	La(1)	N(1A)	58.37(10)	O(4C)	La(2)	O(8C)#1	139.16(12)
N(3B)	La(1)	N(1A)	118.49(10)	O(6C)#1	La(2)	O(8C)#1	76.13(12)
O(1B)	La(1)	N(1B)	60.48(10)				

Symmetry transformations used to generate equivalent atoms: #1 –*x*+2,-*y*+1,-*z*+1

Table S24 Selected least-squares planes data for $[La(\mathbf{L2})_2(hfac)_2]_2[La_2(hfac)_4(O_2CCF_3)_4]$ (**7**).

Least-square planes

Least-squares planes description	Abbreviation	Max. deviation/Å	Atom
Pyridine N1A C1A C2A C3A C4A C5A	PyA	0.0154(12)	N1A
Benzimidazole N4A C11A N3A C12A C13A C14A C15A C16A C17A	BzA	0.0223(11)	N3A
Pyridine N1B C1B C2B C3B C4B C5B	PyB	0.0213(12)	N1B
Benzimidazole N4B C11B N3B C12B C13B C14B C15B C16B C17B	BzB	0.0204(11)	C11B
Hexafluoroacetylacetonate O1H C1H C2H C3H O2H	Hfa I	0.0459(11)	C3H
Hexafluoroacetylacetonate O3H C6H C7H C8H O4H	Hfa II	0.0435 (11)	C8H

Interplanar angles (°)

	PyA	BzA	PyB	BzB	Hfa I
BzA	3.11(3)				
PyB	19.90(3)	22.75(3)			
BzB	25.19(3)	28.28(2)	12.81(3)		
HfaI	57.24(4)	59.93(4)	37.45(4)	38.86(4)	
Hfa II	45.42(4)	43.13(4)	55.62(4)	67.07(4)	78.73(4)

Table S25 Bond Distances ($\delta_{i,j}$), Bond Valences ($v_{\mathrm{Ln,j}}$)[a] and Total Atom Valence (V_{Ln})[b] in the Crystal Structure of [La(**L2**)$_2$(hfac)$_2$]$_2$[La$_2$(hfac)$_4$(O$_2$CCF$_3$)$_4$] (**7**)

Atom[c]	Donor type	$\delta_{\mathrm{La1},j}$ / Å	$v_{\mathrm{La},j}$	
		[La(**L2**)$_2$(hfac)$_2$]$^+$		
N1A	py	2.769	0.253	Average N-heterocyclic
N1B	py	2.788	0.241	0.26 (2)
N3A	bzim	2.728	0.283	
N3B	bzim	2.757	0.262	
O1A	amide	2.549	0.338	Average O-amide
O1B	amide	2.507	0.379	0.36 (3)
O1H	hfac	2.543	0.344	
O2H	hfac	2.550	0.337	Average O-hfa
O3H	hfac	2.571	0.319	0.34 (1)
O4H	hfac	2.537	0.349	
		V_{La1}	3.106	
		[La(hfac)$_4$(O$_2$CCF$_3$)$_4$]$^{2-}$		
O1C	hfac	2.494	0.393	
O2C	hfac	2.497	0.389	
O3C	hfac	2.493	0.394	Average O-hfac
O4C	hfac	2.507	0.379	0.39 (1)
O5C	OAc$_\mathrm{F}$	2.495	0.391	
O6C	OAc$_\mathrm{F}$	2.510	0.376	
O7C	OAc$_\mathrm{F}$	2.460	0.430	Average O-OAc$_\mathrm{F}$
O8C	OAc$_\mathrm{F}$	2.543	0.344	0.39 (4)
		V_{La2}	3.096	

[a] $v_{\mathrm{Ln},j} = e^{\left[\left(R_{\mathrm{Ln},j} - d_{\mathrm{Ln},j}\right)/b\right]}$, whereby $\delta_{\mathrm{Ln},,j}$ is the Ln-donor atom j distance. The valence bond parameters $R_{\mathrm{Ln,N}}$ and $R_{\mathrm{Ln,O}}$ are taken from ref 29e,f and b = 0.37 Å. [b] $V_{\mathrm{Ln}} = \sum_j v_{\mathrm{Ln},j}$. [c] Numbering taken from Fig S13.

Table S26 Ligand-centered absorption and emission properties of **L2**-**L4** and of their complexes $[Ln_m(\mathbf{L}\boldsymbol{k})(hfac)_{3m}]$ in the solid state.

Compound	Absorption /cm^{-1} [a] $^1\pi^* \leftarrow {}^1\pi$	Emission /cm^{-1} [b] $^1\pi^* \rightarrow {}^1\pi$	Emission /cm^{-1} [b] $^3\pi^* \rightarrow {}^1\pi$	Lifetime /ms τ ($^3\pi^*$)
L2	31445	29110 sh	21280 sh	3.9(2)
		27780	20000	
		26455 sh	18870 sh	
L3	29585	28250 sh	20408 sh	1.7(1)
		26990	19420	
		23725		
L4	30395	27780 sh	20000 sh	1.4(1)
		26665	19050	
		21645 sh		
[Lu(**L2**)(hfac)$_3$]	31545	25350	20830 sh	1.08(6)
			19420	
			18180 sh	
[Gd(**L2**)(hfac)$_3$]	31545	24875	21740 sh	1.06(5)
	28490 sh		20620	
			19610 sh	
			18180 sh	
[Eu(**L2**)(hfac)$_3$]	31750	[c]	[c]	-
	28490 sh			
[Lu$_2$(**L3**)(hfac)$_6$]	31350	24875	20620 sh	2.4(2)
	27780 sh		19420	
			18350 sh	
[Gd$_2$(**L3**)(hfac)$_3$]	31446	24783	21276 sh	0.19(1)
	27933 sh		19802	
			18518 sh	
[Eu$_2$(**L3**)(hfac)$_6$]	31650	[c]	[c]	-
	27470 sh			
[Gd$_3$(**L4**)(hfac)$_9$]	31250	23980	20620 sh	0.20(3)
	26525 sh		19230	
			17860 sh	
[Eu$_3$(**L4**)(hfac)$_9$]	31850	[c]	[c]	-
	26670 sh			

[a] Reflectance spectra recorded from MgO matrices at 293 K, sh = shoulder. [b] Recorded at 77 K with $\bar{\nu}_{exc}$ = 30300 cm^{-1}. [c] Quenched by quantitative transfer onto Eu(III).

Table S27 Integral intensities of $^5D_0 \rightarrow {}^7F_J$ ($J = 0 - 4$) transitions in Eu^{III} complexes.[a]

Compound	$\int_{0\text{-}0}$	$\int_{0\text{-}1}$	$\int_{0\text{-}2}$	$\int_{0\text{-}3}$	$\int_{0\text{-}4}$	$\int_{tot}/\int_{0\text{-}1}$
[Eu(**L2**)(hfac)$_3$]	0.14	1.0	12.64	0.28	1.39	15.46
[Eu$_2$(**L3**)(hfac)$_6$]	0.12	1.0	12.18	0.25	1.34	14.89
[Eu$_3$(**L4**)(hfac)$_9$]	0.10	1.0	11.34	0.19	1.32	13.94

[a] Experimental error, ±5%.

Table S28 ^{1}H NMR shifts of aromatic part (in ppm with respect to TMS) for the ligand **L2** and its complexes [Ln(**L2**)(hfac)$_3$] in CD_3CN at 293 K (Ln = La, Y, Lu).

	H1	H2	H3	H4	H5	H6	H7	H-hfac
L2	7.58	7.36	7.30	7.74	8.37	8.02	7.51	-
[La(**L2**)$_2$(hfac)$_3$]	7.65	7.44	7.30	8.03	8.21	8.35	7.99	5.90
[Y(**L2**)(hfac)$_3$]	7.63	7.42	7.27	8.20	8.25	8.34	8.01	5.87
[Y(**L2**)(hfac)$_2$]$^+$	7.72	7.50	7.40	8.11	8.44	8.44	8.09	5.87
[Lu(**L2**)(hfac)$_3$]	7.64	7.43	7.30	8.22	8.27	8.35	8.04	5.87
[Lu(**L2**)(hfac)$_2$]$^+$	7.71	7.51	7.40	8.07	8.36	8.46	8.13	6.14

Table S29 ^{19}F NMR shifts (in ppm with Respect to Hexafluorobenzene) for the complexes [Ln(**L2**)(hfac)$_3$] at 293 K (Ln = La, Eu, Y, Lu).

	δ/$CDCl_3$	δ/CD_3CN
$[La(\mathbf{L2})_2(hfac)_2]^+$	-	-77.06
$[La_2(hfac)_4(CF_3COO)_4]^{2-}$	-	-77.41
[La(**L2**)(hfac)$_3$]	-76.78	-77.41
[Eu(**L2**)(hfac)$_3$]		-79.93
[Y(**L2**)(hfac)$_3$]	-76.86	-77.48
$[Y(\mathbf{L2})(hfac)_2]^+$	-	-77.21
[Lu(**L2**)(hfac)$_3$]	-76.93	-77.47
$[Lu(\mathbf{L2})(hfac)_2]^+$	-	-77.14

Table S30 Cumulative thermodynamic formation constants $\log(\beta_{m,1}^{\mathrm{Ln(hfac)3,}\mathbf{Lk}})$, associated intermolecular microscopic affinities ($\Delta G_{\mathrm{inter}}^{\mathrm{Ln,N3}} = -RT\ln\left(f_{\mathrm{N3}}^{\mathrm{Ln}}\right)$ and $\Delta G_{\mathrm{inter}}^{\mathrm{Ln,N2O}} = -RT\ln\left(f_{\mathrm{N2O}}^{\mathrm{Ln}}\right)$ in kJ/mol) and intermetallic ($\Delta E_{1-2}^{\mathrm{Ln,Ln}} = -RT\ln\left(u_{1-2}^{\mathrm{Ln,Ln}}\right)$ and $\Delta E_{1-3}^{\mathrm{Ln,Ln}} = -RT\ln\left(u_{1-3}^{\mathrm{Ln,Ln}}\right)$ in kJ/mol) interactions obtained for $[\mathrm{Ln}_m(\mathbf{Lk})(\mathrm{hfac})_{3m}]$ (Ln = La, Eu, Y, Lu; CH_3CN, 298 K).

Metal	La	Eu	Y	Lu	Reference
$\log(\beta_{1,1}^{\mathrm{Ln(hfac)3,}\mathbf{L1}})$	5.7(1)	5.94(9)	5.15(5)	4.3(3)	18
$\log(\beta_{1,1}^{\mathrm{Ln(hfac)3,}\mathbf{L2}})$	5.66(6)	6.3(1)	5.47(8)	5.57(6)	This work
$\log(\beta_{1,1}^{\mathrm{Ln(hfac)3,}\mathbf{L3}})$	5.93(8)	6.6(1)	5.79(7)	4.02(9)	This work
$\log(\beta_{2,1}^{\mathrm{Ln(hfac)3,}\mathbf{L3}})$	10.95(6)	11.9(1)	10.87(6)	7.34(5)	This work
$\log(\beta_{1,1}^{\mathrm{Ln(hfac)3,}\mathbf{L4}})$	4.5(1)	5.40(7)	3.9(2)	*5.52(9)* [a]	This work
$\log(\beta_{2,1}^{\mathrm{Ln(hfac)3,}\mathbf{L4}})$	9.88(7)	10.70(7)	9.50(1)	*11.6(1)* [a]	This work
$\log(\beta_{3,1}^{\mathrm{Ln(hfac)3,}\mathbf{L4}})$	14.01(9)	16.25(6)	13.9(1)	*17.1(1)* [a]	This work
$\log(f_{\mathrm{N2O}}^{\mathrm{Ln,}\mathbf{L2}})$/ $\Delta G_{\mathrm{inter}}^{\mathrm{Ln,N2O,}\mathbf{L2}}$	5.2(2)/-30(1)	5.8(2)/-33(1)	5.0(3)/-29(1)	-	This work
$\log(f_{\mathrm{N2O}}^{\mathrm{Ln}})/\Delta G_{\mathrm{inter}}^{\mathrm{Ln,N2O}}$	4.8(2)/-27(1)	4.9(2)/-30(1)	4.5(3)/-26(1)	-	This work
$\log(f_{\mathrm{N3}}^{\mathrm{Ln,}\mathbf{L1}})/\Delta G_{\mathrm{inter}}^{\mathrm{Ln,N3,}\mathbf{L1}}$	5.2(1)/-30(1)	5.5(1)/-31(1)	4.7(1)/-27(1)	-	18
$\log(f_{\mathrm{N3}}^{\mathrm{Ln}})/\Delta G_{\mathrm{inter}}^{\mathrm{Ln,N3}}$	3.1(2)/-18(1)	3.2(2)/-18(1)	2.5(3)/-14(1)	-	This work
$\log(u_{1-2}^{\mathrm{Ln,Ln}})/\Delta E_{1-2}^{\mathrm{Ln,Ln}}$	0.4(2)/-2(1)	1.1(2)/-6(1)	0.9(3)/-5(1)	-	This work
$\log(u_{1-3}^{\mathrm{Ln,Ln}})/\Delta E_{1-3}^{\mathrm{Ln,Ln}}$	-0.9(2)/5(1)	-0.4(2)/2(1)	-0.8(3)/5(1)	-	This work

[a] Due to major difficulties during the fitting process, these values are only mere estimates (see text).

Table S31 Cumulative thermodynamic formation constants $\log(\beta_{m,1}^{\mathrm{Ln(NO3)3,}\mathbf{Lk}})$, associated intermolecular microscopic affinities ($\Delta G_{\mathrm{inter}}^{\mathrm{Ln,N3}} = -RT\ln\left(f_{\mathrm{N3}}^{\mathrm{Ln}}\right)$ and $\Delta G_{\mathrm{inter}}^{\mathrm{Ln,N2O}} = -RT\ln\left(f_{\mathrm{N2O}}^{\mathrm{Ln}}\right)$ in kJ/mol) and intermetallic ($\Delta E_{1-2}^{\mathrm{Ln,Ln}} = -RT\ln\left(u_{1-2}^{\mathrm{Ln,Ln}}\right)$ and $\Delta E_{1-3}^{\mathrm{Ln,Ln}} = -RT\ln\left(u_{1-3}^{\mathrm{Ln,Ln}}\right)$ in kJ/mol) interactions obtained for $[\mathrm{Ln}_m(\mathbf{L}\boldsymbol{k})(\mathrm{NO_3})_{3m}]$ (Ln = La, Eu, Y, Lu; CH_3CN, 298 K).

Metal	La	Eu	Y	Lu	Reference
$\log(\beta_{1,1}^{\mathrm{Ln(NO3)3,}\mathbf{L2}})$	5.77(6)	5.27(9)	5.99(9)	6.06(9)	19
$\log(\beta_{1,1}^{\mathrm{Ln(NO3)3,}\mathbf{L3}})$	5.09(9)	5.49(4)	5.69(8)	5.79(9)	19
$\log(\beta_{2,1}^{\mathrm{Ln(NO3)3,}\mathbf{L3}})$	9.20(8)	9.42(6)	10.12(9)	10.36(9)	19
$\log(\beta_{1,1}^{\mathrm{Ln(NO3)3,}\mathbf{L4}})$	6.4(2)	6.8(2)	6.8(2)	*7.9(2)* [a]	This work
$\log(\beta_{2,1}^{\mathrm{Ln(NO3)3,}\mathbf{L4}})$	12.3(2)	12.7(3)	12.7(2)	*14.2(3)* [a]	This work
$\log(\beta_{3,1}^{\mathrm{Ln(NO3)3,}\mathbf{L4}})$	17.3(2)	17.4(3)	17.8(2)	*19.8(3)* [a]	This work
$\log(f_{\mathrm{N2O(}\mathbf{L2}\mathrm{)}}^{\mathrm{Ln}})/\Delta G_{\mathrm{inter}}^{\mathrm{Ln,N2O,}\mathbf{L2}}$	5.3(2)/-30(1)	4.8(2)/-27(1)	5.6(3)/-32(2)	-	19
$\log(f_{\mathrm{N2O}}^{\mathrm{Ln}})/\Delta G_{\mathrm{inter}}^{\mathrm{Ln,N2O}}$	4.5(1)/-25.6(4)	4.7(1)/-26.9(3)	4.9(3)/-28.3(4)	-	This work
$\log(f_{\mathrm{N3(}\mathbf{L1}\mathrm{)}}^{\mathrm{Ln,}})/\Delta G_{\mathrm{inter}}^{\mathrm{Ln,N3,}\mathbf{L1}}$	4.2(2)/-24.1(8)	4.2(2)/-24.2(8)	4.4(2)/-25.1(9		47
$\log(f_{\mathrm{N3}}^{\mathrm{Ln}})/\Delta G_{\mathrm{inter}}^{\mathrm{Ln,N3}}$	6.3(1)/-35.5(1)	6.2(1)/-35.5(1)	6.2(1)/-35.5(1)	-	This work
$\log(u_{1-2}^{\mathrm{Ln,Ln}})/\Delta E_{1-2}^{\mathrm{Ln,Ln}}$	-0.8(1)/4.6(2)	-0.8(2)/5.4(4)	-0.8(1)/4.4(2)	-	This work
$\log(u_{1-3}^{\mathrm{Ln,Ln}})/\Delta E_{1-3}^{\mathrm{Ln,Ln}}$	2.3(1)/-13(1)	2.2(3)/-12(2)	1.8(1)/-10(1)	-	This work

[a] Due to major difficulties during the fitting process, these values are only mere estimates (see text).

Table S32 ^{1}H NMR shifts of aromatic part (in ppm with respect to TMS) for the ligand **L2** and its complexes [Ln(**L2**)(hfac)$_3$] in $CDCl_3$ at 293 K (Ln = La, Y, Lu).

Compound	H1	H2	H3	H4	H5	H6	H7	H-hfac
L2	7.47	7.37	7.33	7.87	8.44	7.96	7.57	-
[La(**L2**)(hfac)$_3$]	7.41	7.41	7.34	8.19	7.95	8.19	7.72	5.85
[Y(**L2**)(hfac)$_3$]	7.39	7.39	7.32	8.36	7.97	8.19	7.76	5.84
[Lu(**L2**)(hfac)$_3$]	7.40	7.40	7.33	8.38	8.02	8.19	7.77	5.82

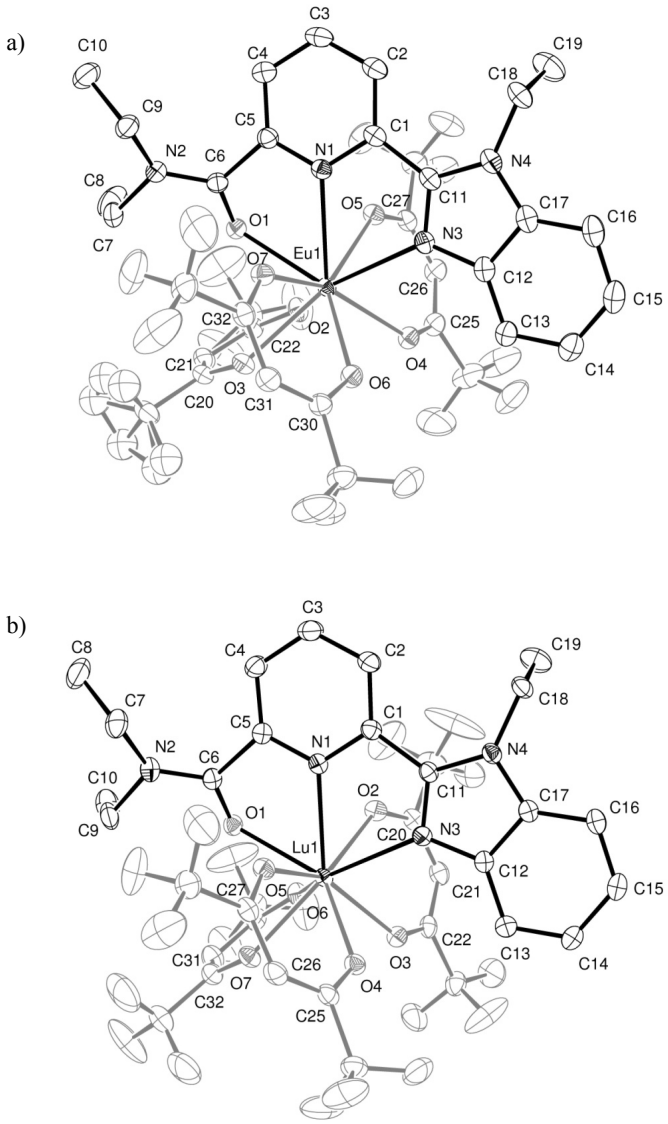

Figure S1 Molecular structures with partial numbering schemes of the assymetric units for a) [Eu(**L2**)(hfac)$_3$] and b) [Lu(**L2**)(hfac)$_3$] in the crystal structures of **2** and **5** (thermal ellipsoids are represented at the 30% probability level). Hydrogen atoms are omitted for clarity.

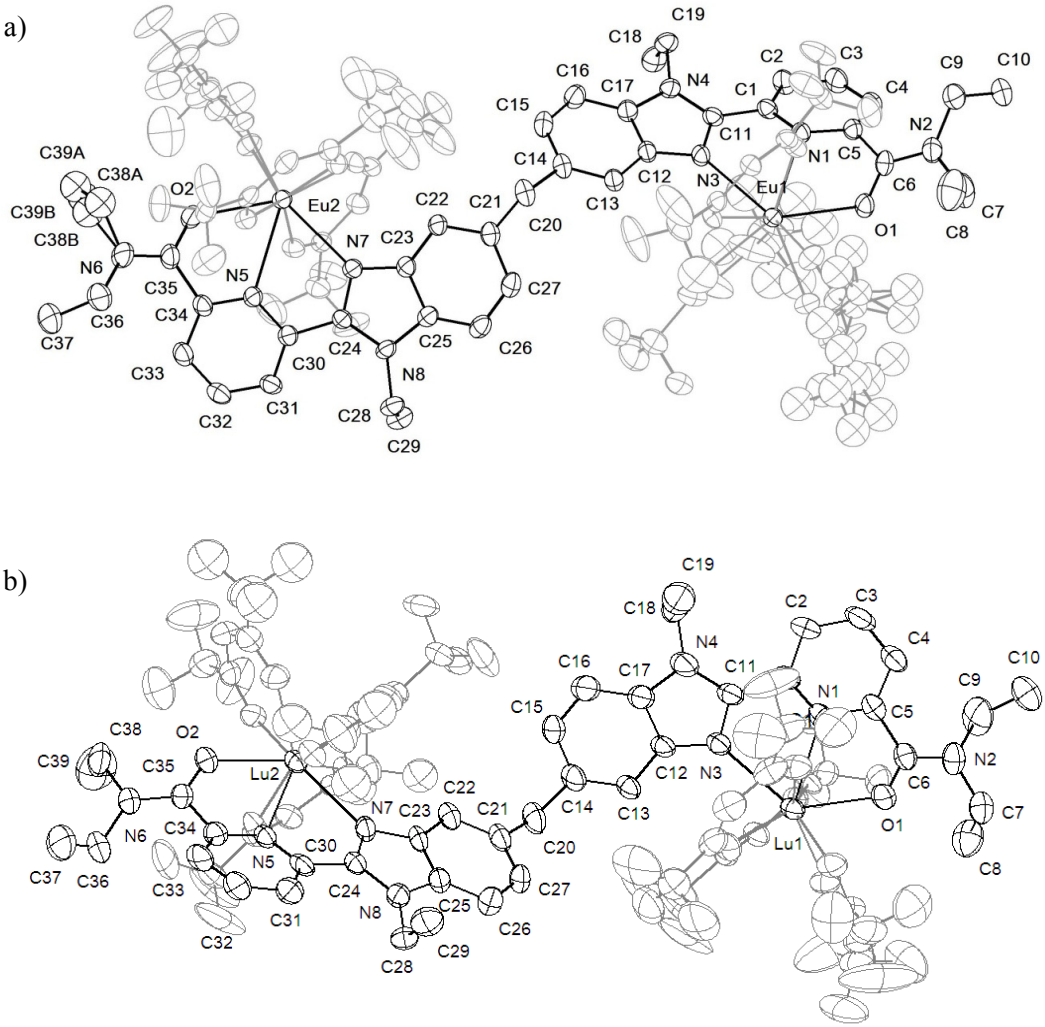

Figure S2 Molecular structures with partial numbering schemes of the assymetric units for a) $[Eu_2(\mathbf{L3})(hfac)_6]$ and b) $[Lu_2(\mathbf{L3})(hfac)_6]$ in the crystal structures of **3** and **6** (thermal ellipsoids are represented respectively at the 30% and 50% probability levels). Hydrogen atoms are omitted for clarity.

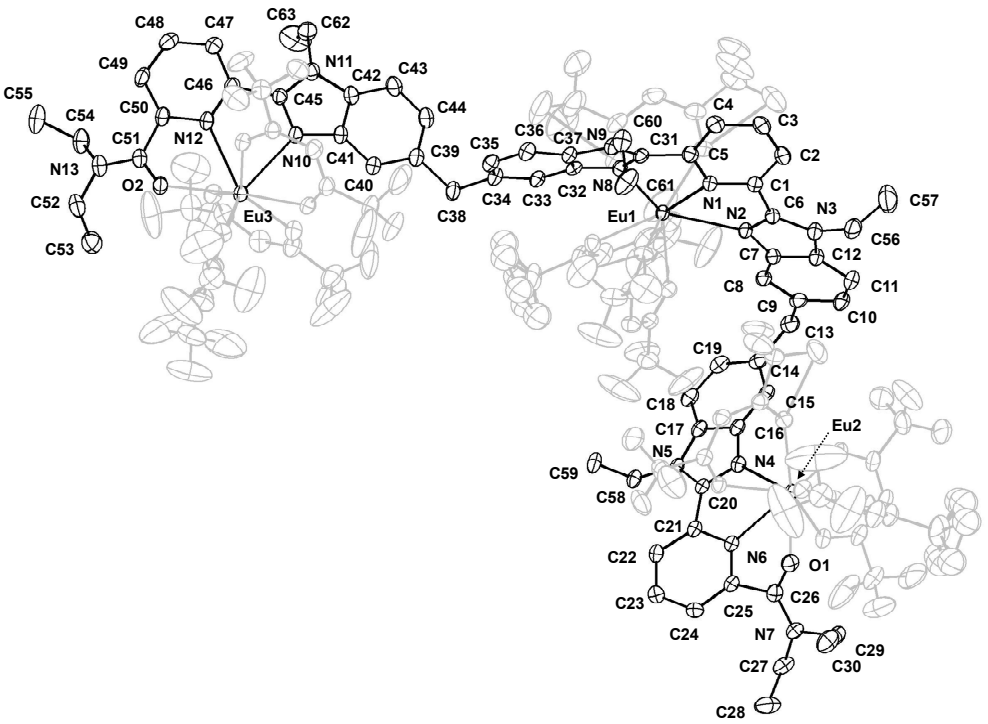

Figure S3 Molecular structure with partial numbering scheme of the assymetric unit for [Eu_3(**L4**)(hfac)$_9$] in the crystal structure of **4** (thermal ellipsoids are represented at the 30% probability level). Hydrogen atoms are omitted for clarity.

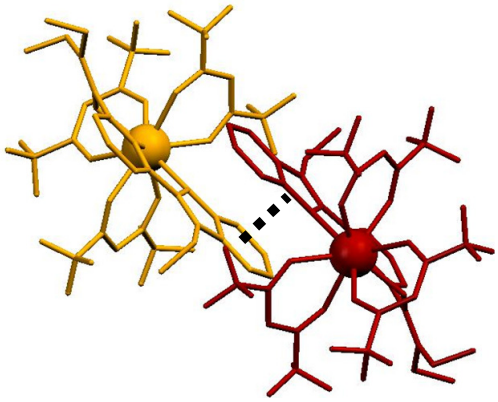

Figure S4 Intermolecular π-stacking benzimidazole···benzimidazole interactions (d = 3.35Å) found in [Lu(**L2**)(hfac)$_3$] (**5**) involving neighbouring molecules related by inversion centres.

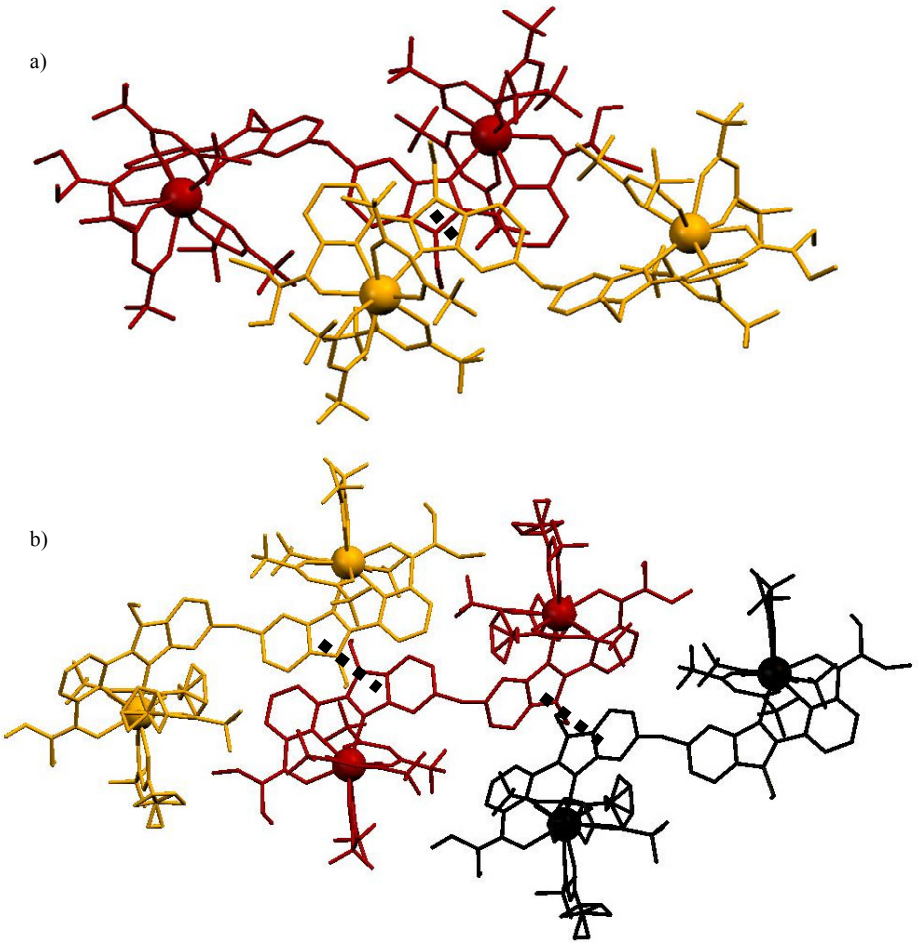

Figure S5 Intermolecular π-stacking benzimidazole···benzimidazole interactions found in a) $[Eu_2(\mathbf{L3})(hfac)_6]$ (**3**) (d = 3.50Å) and b) $[Lu_2(\mathbf{L3})(hfac)_6]$ (**6**) (d = 3.60Å) involving neighbouring molecules related by inversion centres.

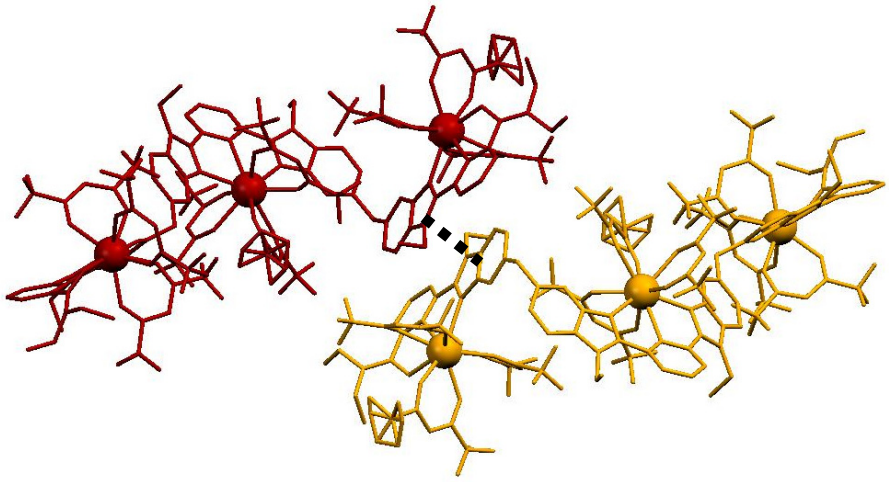

Figure S6 Intermolecular π-stacking benzimidazole···benzimidazole interactions (d = 3.32Å) interactions found in $[Eu_3(\mathbf{L4})(hfa)_9]$ (**4**) involving neighbouring molecules related by inversion centres.

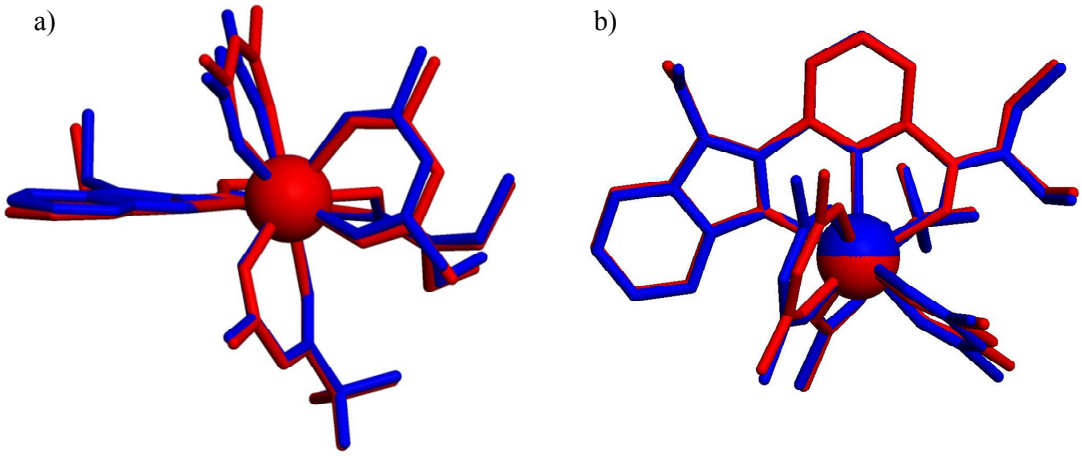

Figure S7 Superimposition of the molecular structures of [Eu(**L2**)(hfac)$_3$] (red) and [Lu(**L2**)(hfac)$_3$] (blue). Perspective views a) along and b) perpendicular to the pyridine plane of the tridentate ligand. Hydrogen and fluorine atoms are omitted for clarity.

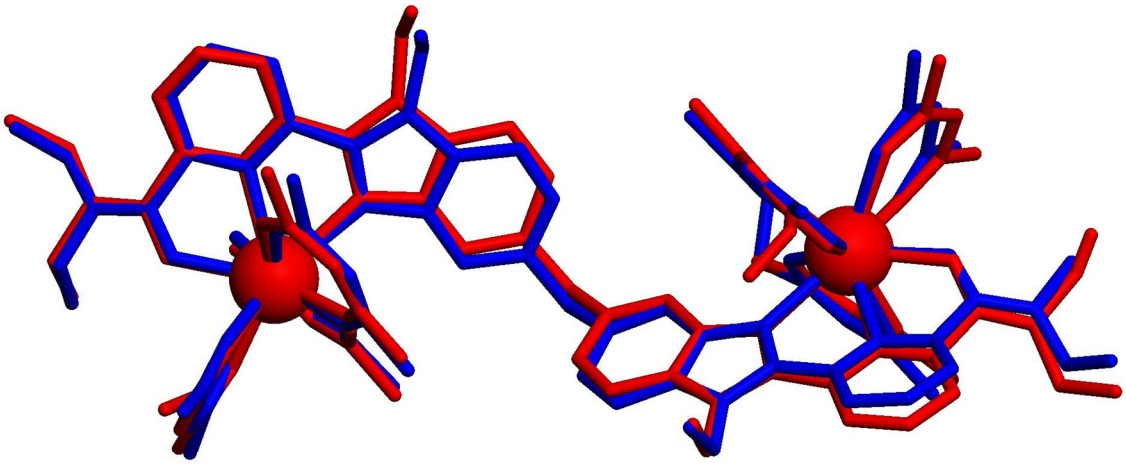

Figure S8 Superimposition of the molecular structures of [Eu$_2$(**L3**)(hfac)$_6$] (red) and [Lu$_2$(**L3**)(hfac)$_6$] (blue). Hydrogen and fluorine atoms are omitted for clarity.

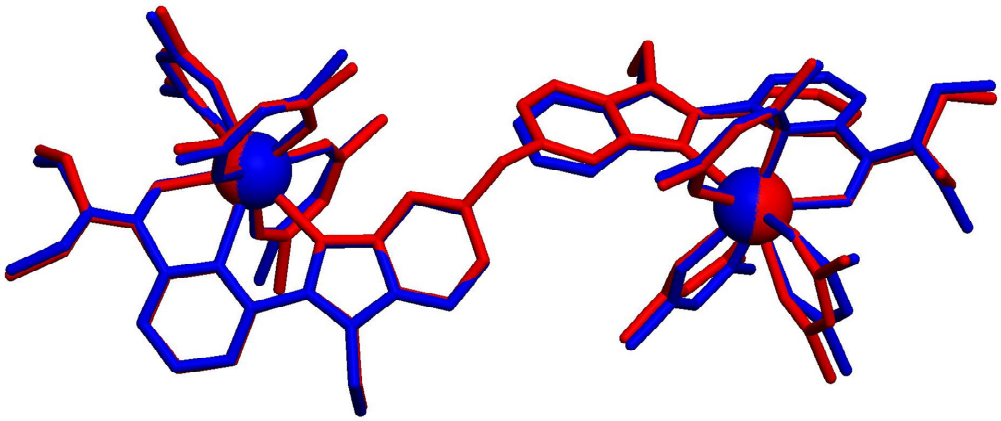

Figure S9 Superimposition of the molecular structures of $[Eu_2(\mathbf{L3})(hfac)_6]$ (red) and $[Eu_2(\mathbf{L2})(hfac)_3]$ (twice, blue). Hydrogen and fluorine atoms are omitted for clarity.

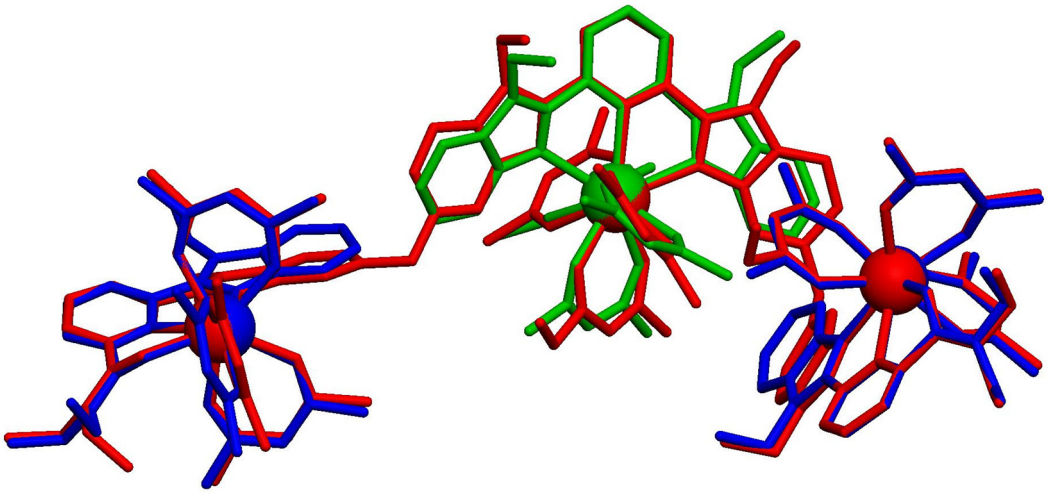

Figure S10 Superimposition of the molecular structures of $[Eu_3(\mathbf{L4})(hfac)_9]$ (red) and $[Eu_2(\mathbf{L2})(hfac)_3]$ (twice, blue) and $[Eu(\mathbf{L1})(hfac)_3]$ (green). Hydrogen and fluorine atoms are omitted for clarity.

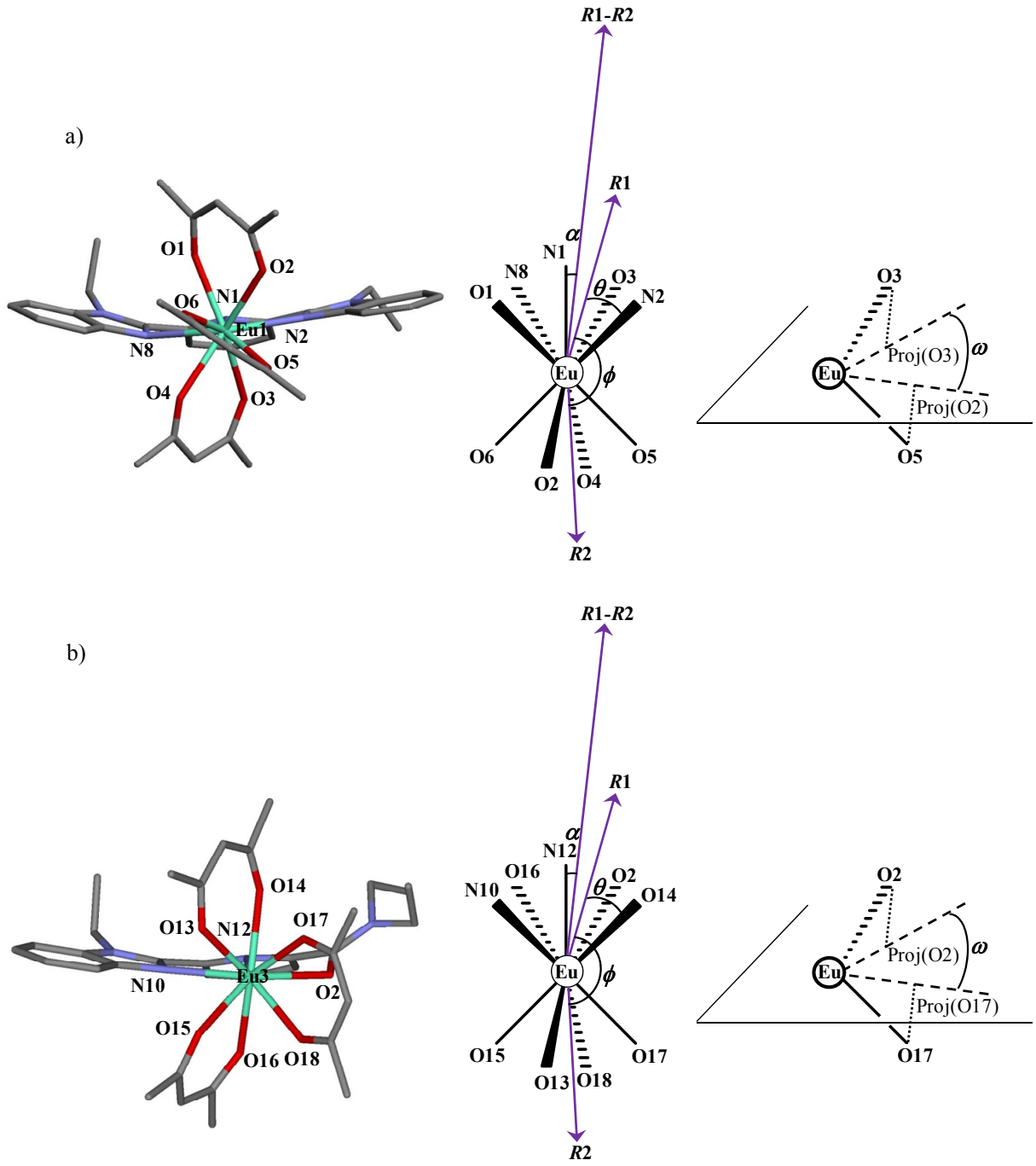

Figure S11 Perspective views along the Eu-N(pyridine) direction (left) and associated angles α, ϕ, θ and ω characterizing the pseudo-monocapped square antiprismatic geometry adopted by the coordination spheres around Eu^{III} in a) the central $[Eu(N_3)(hfac)_3]$ unit and b) the distal $[Eu(N_2O)(hfac)_3]$ unit in the trinuclear $[Eu_3(\mathbf{L4})(hfac)_9]$. Hydrogen and fluorine atoms are omitted for clarity.

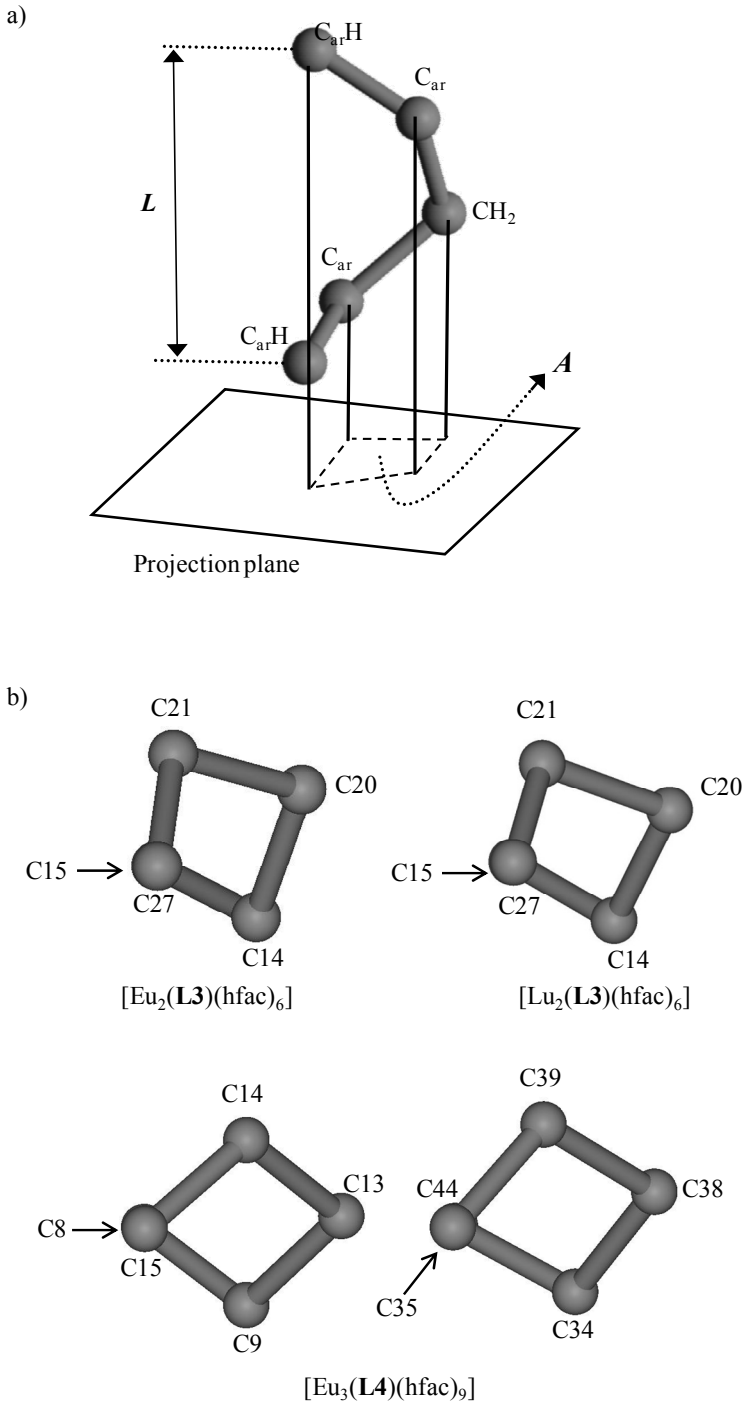

Figure S12 a) Analysis of the helicity of a five-atoms crooked line proposed by Brewster (*L* is the end to end distance of the helix, *A* is the area of the subtended figure in the projection plane and *D* is the total length of the crooked line).[30] b) Subtended geometrical figures obtained in the projection plane for $[Eu_2(\mathbf{L3})(hfac)_6]$, $[Lu_2(\mathbf{L3})(hfac)_6]$ and $[Eu_3(\mathbf{L4})(hfac)_9]$.

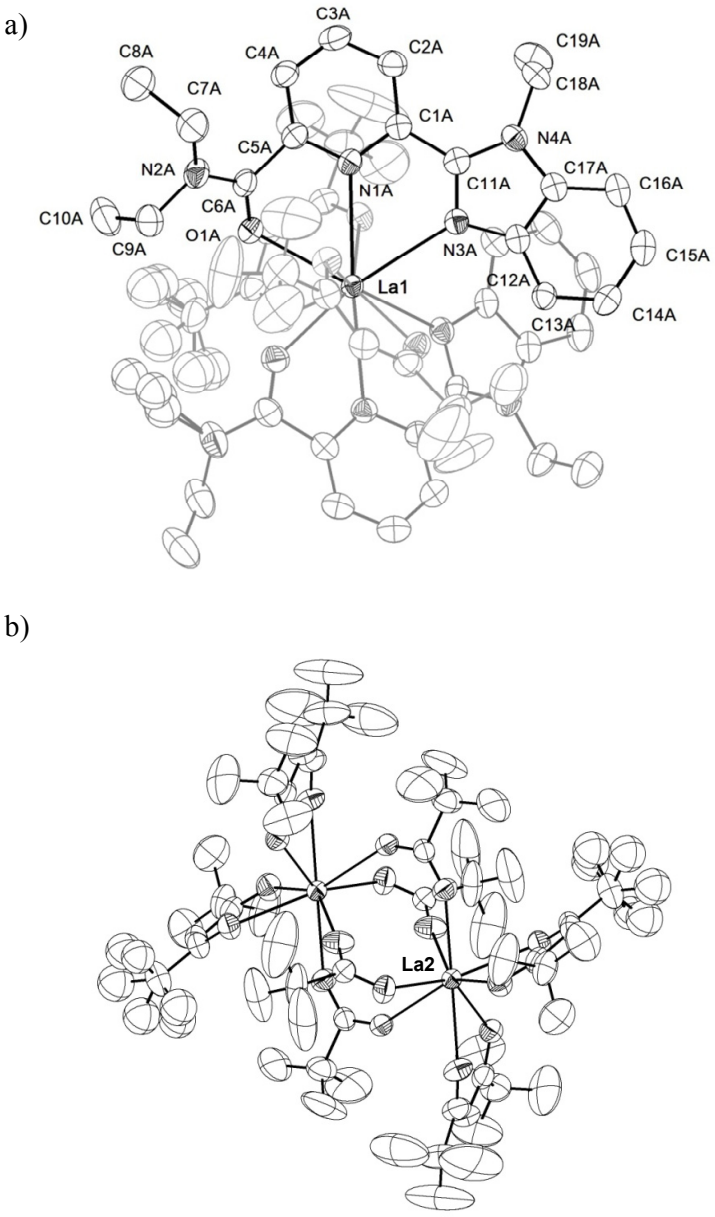

Figure S13 Molecular structure with partial numbering scheme of a) $[La(\mathbf{L2})_2(hfac)_2]^+$ and b) $[La_2(hfac)_4(O_2CCF_3)_4]^{2-}$ in the crystal structure of **7** (thermal ellipsoids are represented at the 50% probability level). Hydrogen atoms are omitted for clarity.

a)

b)

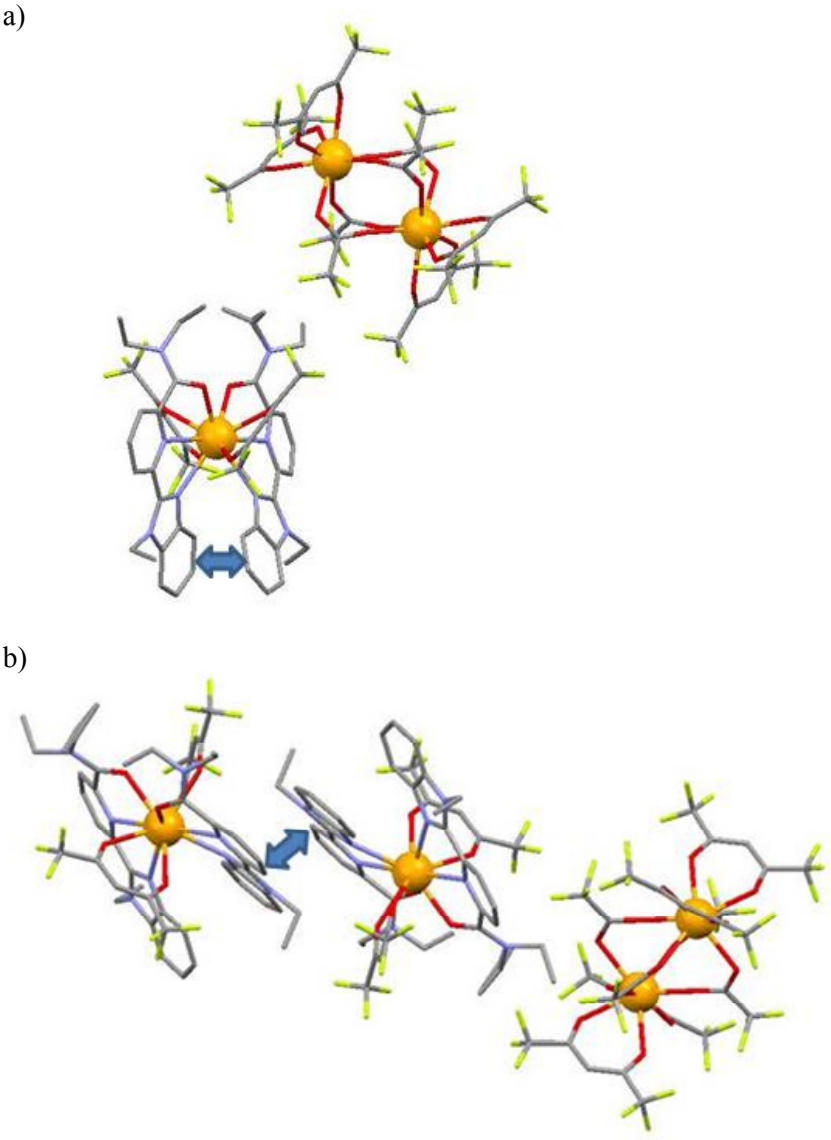

Figure S14 a) Intramolecular (interplanar angle = 28° *d* = 3.7 Å and b) intermolecular π-stacking benzimidazole···benzimidazole interactions (3.36(1) Å) found in $[La(\mathbf{L2})_2(hfac)_2]^+$ in the crystal structure of **7**.

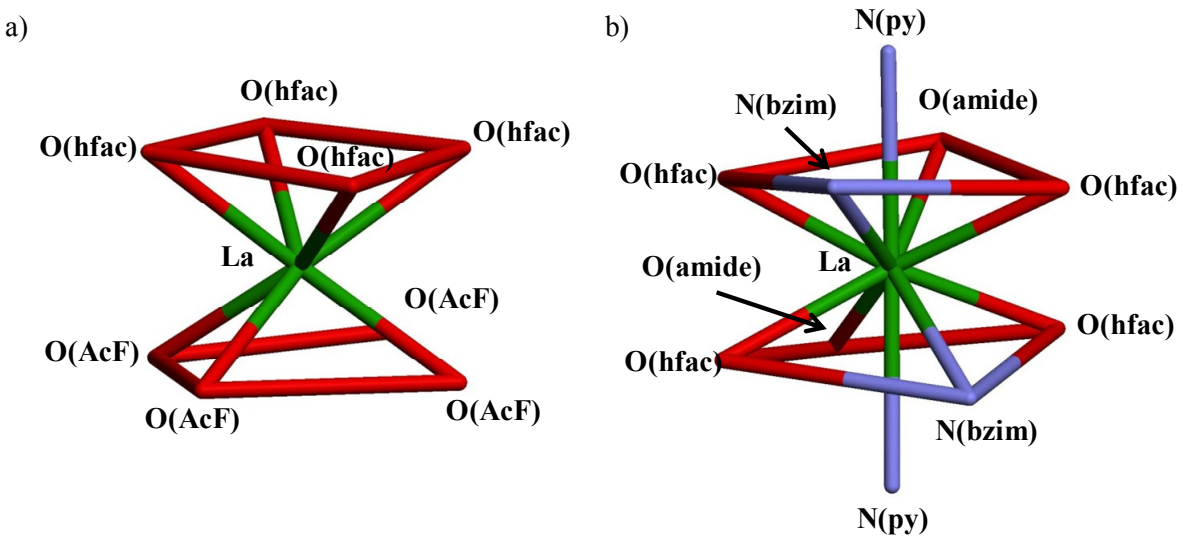

Figure S15 Coordination spheres around La^{III} in a) $[La_2(hfac)_4(O_2CCF_3)_4]^{2-}$ (pseudo-square antiprism) and b) $[La(\mathbf{L2})_2(hfac)_2]^{+}$ (pseudo-bicapped square antiprism) in the crystal structure of **7**.

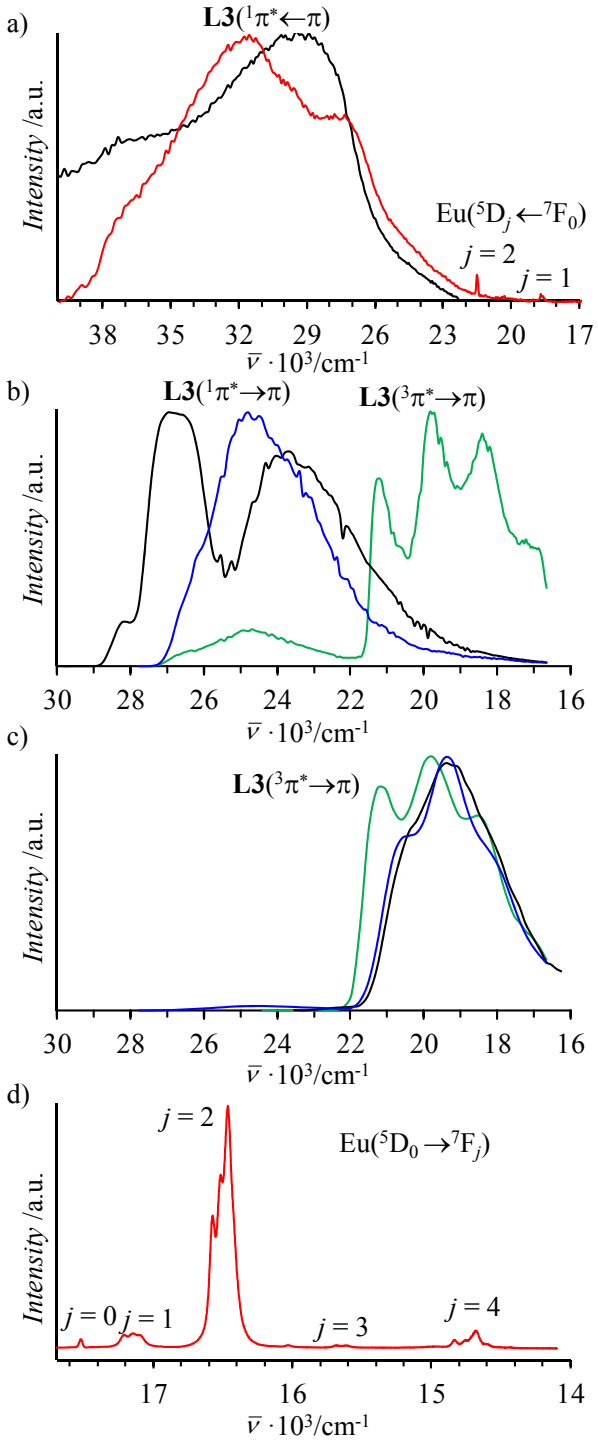

Figure S16 Solid state a) reflectance absorption spectra (293 K), b) emission spectra ($\bar{\nu}_{exc}$ = 30300-29500 cm^{-1}, 77 K), c) phosphorescence spectra ($\bar{\nu}_{exc}$ = 30300-29500 cm^{-1}, delay time after excitation flash 5 μs, 77 K) d) luminescence spectra ($\bar{\nu}_{exc}$ = 28170 cm^{-1} at 293 K) recorded for **L3** (black traces), $[Lu_2(\mathbf{L3})(hfac)_6]$ (blue traces), $[Gd_2(\mathbf{L3})(hfac)_6]$ (green traces) and $[Eu_2(\mathbf{L3})(hfac)_6]$ (red traces).

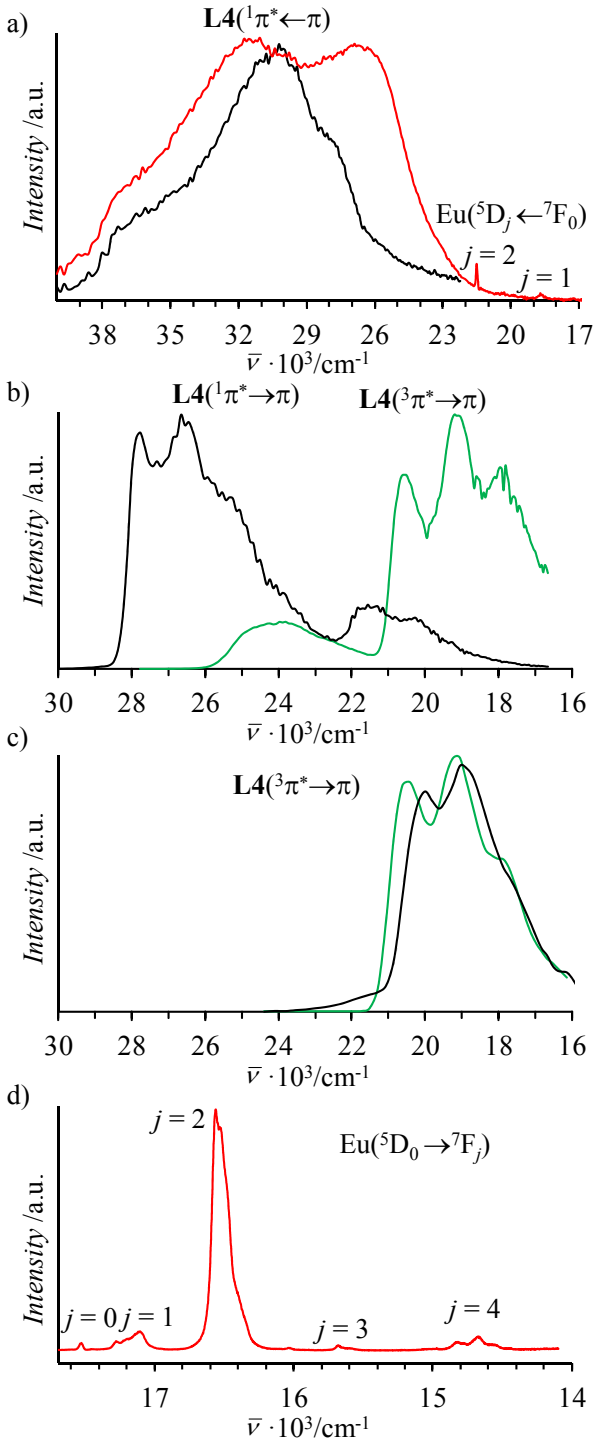

Figure S17 Solid state a) reflectance absorption spectra (293 K), b) emission spectra ($\bar{\nu}_{exc}$ = 30300-29500 cm^{-1}, 77 K), c) phosphorescence spectra ($\bar{\nu}_{exc}$ = 30300-29500 cm^{-1}, delay time after excitation flash 5 μs, 77 K) d) luminescence spectra ($\bar{\nu}_{exc}$ = 28170 cm^{-1} at 293 K) recorded for **L4** (black traces), $[Gd_3(\mathbf{L4})(hfac)_9]$ (green traces) and $[Eu_3(\mathbf{L4})(hfac)_9]$ (red traces).

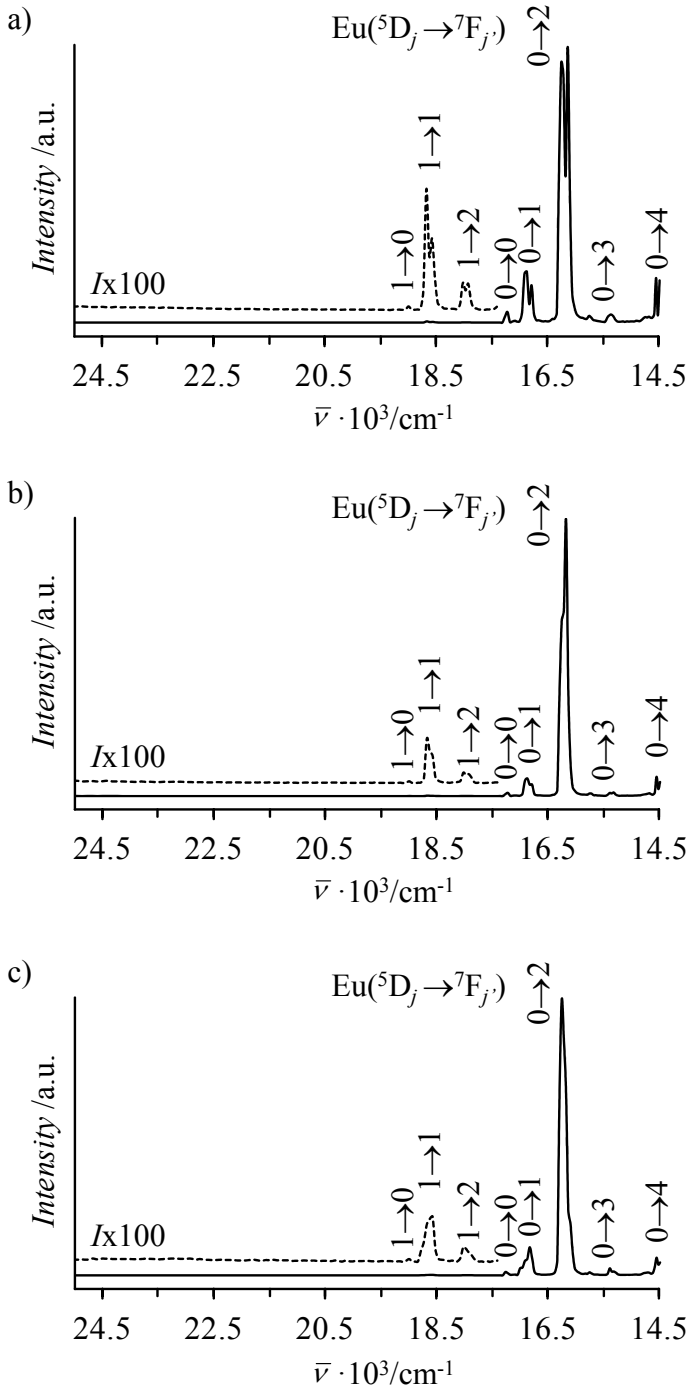

Figure S18 Luminescence spectra ($\bar{\nu}_{exc}$ = 29000 cm^{-1}, solid state 77 K) recorded for a) [Eu(**L2**)(hfac)$_3$], b) [Eu$_2$(**L3**)(hfac)$_6$] and c) [Eu$_3$(**L4**)(hfac)$_9$].

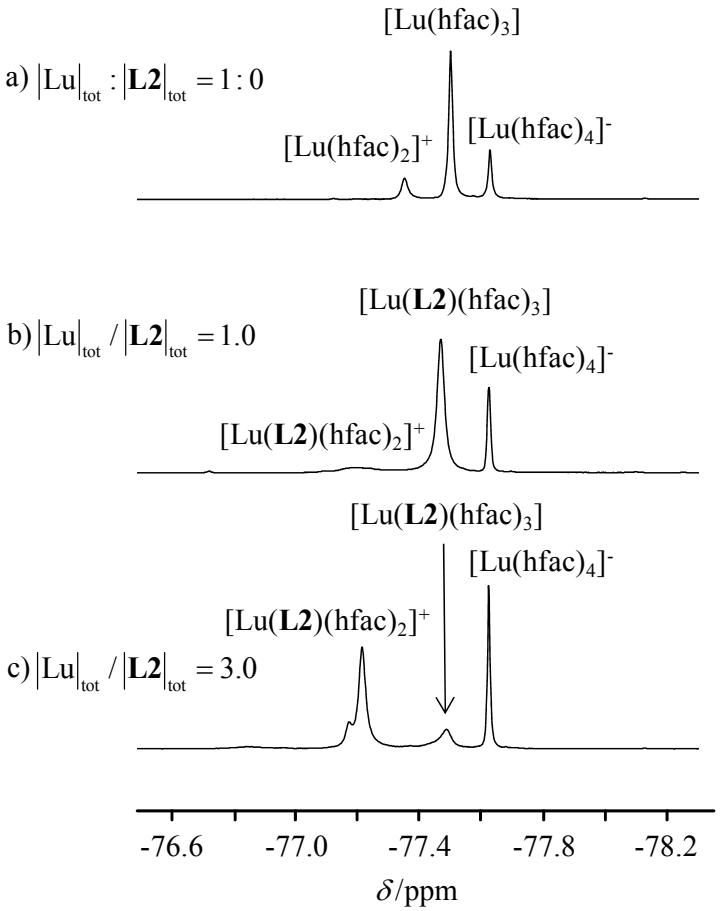

Figure S19 Selected ^{19}F NMR spectra recorded during the titration of **L2** with [Lu(hfac)$_3$(diglyme)] in CD_3CN at 293 K. a) Lu:**L2** = 1:0, b) Lu:**L2** = 1:1 and c) Lu:**L2** = 3:1.

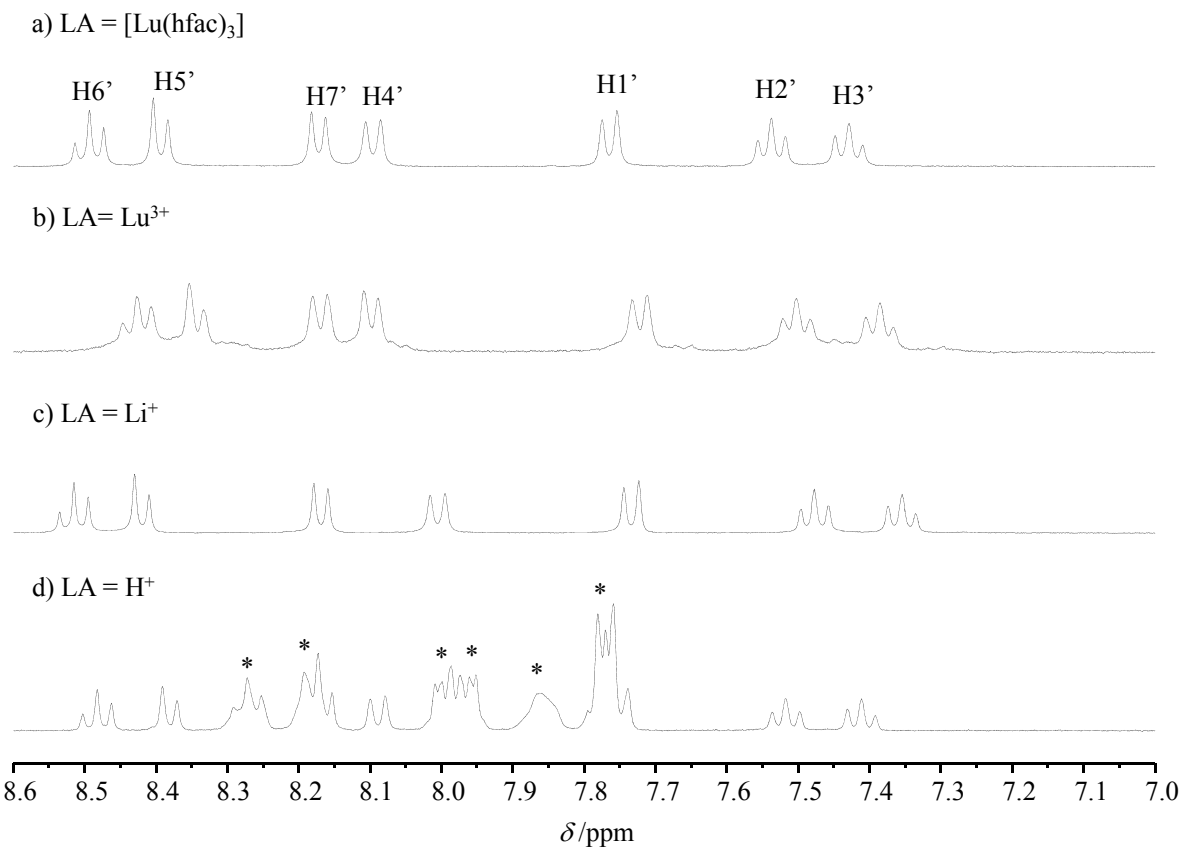

Figure S20 ^{1}H NMR spectra recorded for [Lu(**L2**)(hfac)$_2$]$^+$ in CD_3CN at 293 K prepared by reacting [Lu(**L2**)(hfac)$_3$] with various Lewis acids (LA). a) LA = [Lu(hfac)$_3$] obtained from [Lu(hfac)$_3$(diglyme)], b) LA = Lu^{3+} obtained from [Lu(CF_3SO_3)$_3$(diglyme)], c) LA = Li^+ obtained from $LiClO_4$ and d) LA = H^+ obtained form CF_3SO_3H (the signals with an asterisk are those of the protonated ligand).

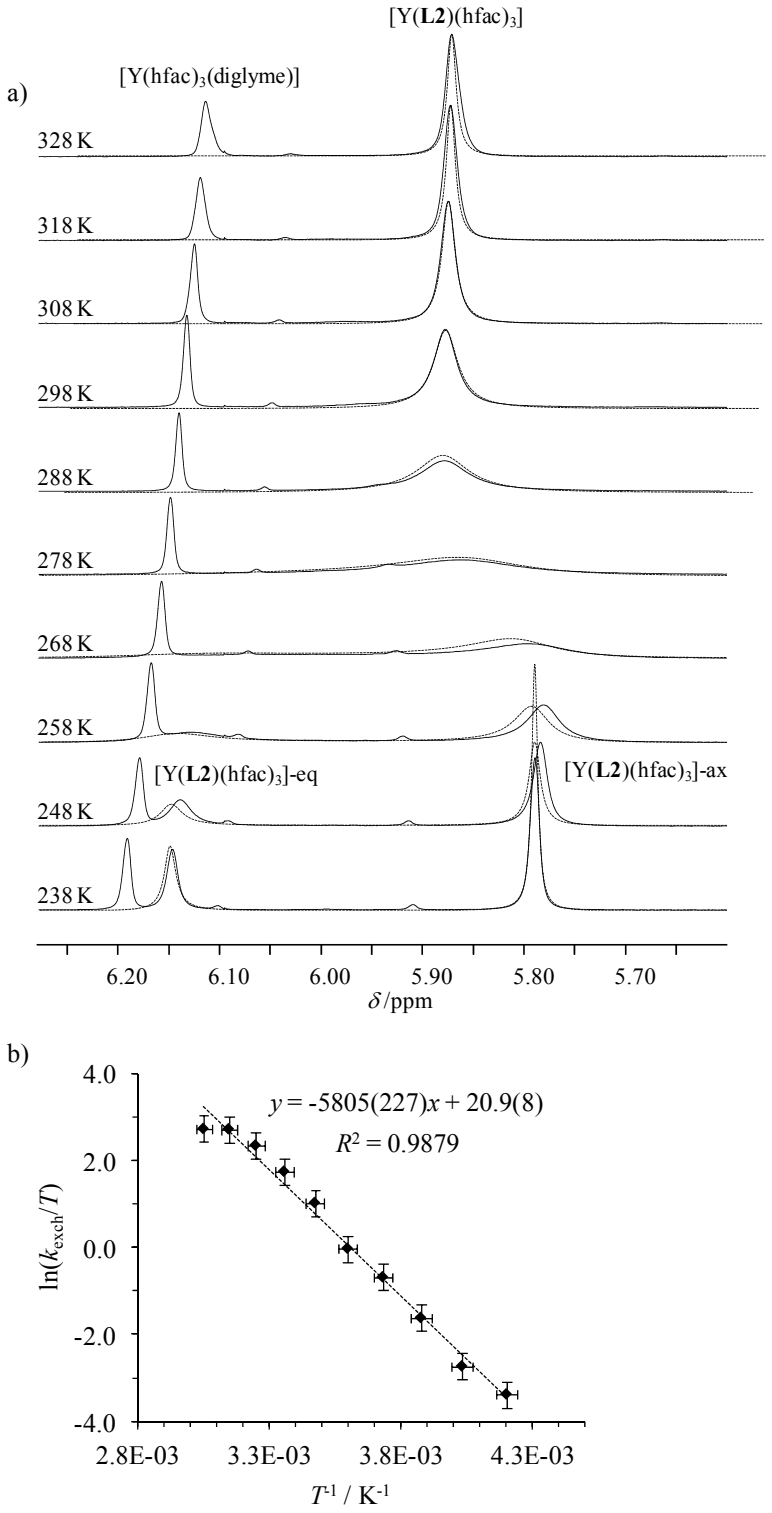

Figure S21 a) Experimental (full line) and simulated (dotted line) variable temperature ^{1}H NMR spectra recorded for [Ln(**L2**)(hfac)$_3$] in CD_3CN and showing the signals of the protons connected to the bound hfac anions (an excess of [Y(diglyme)(hfac)$_3$] was used as a reference). b) Eyring plots of the first-order kinetic rate constants calculated for the dynamic exchange between axial and equatorial hfac anion.

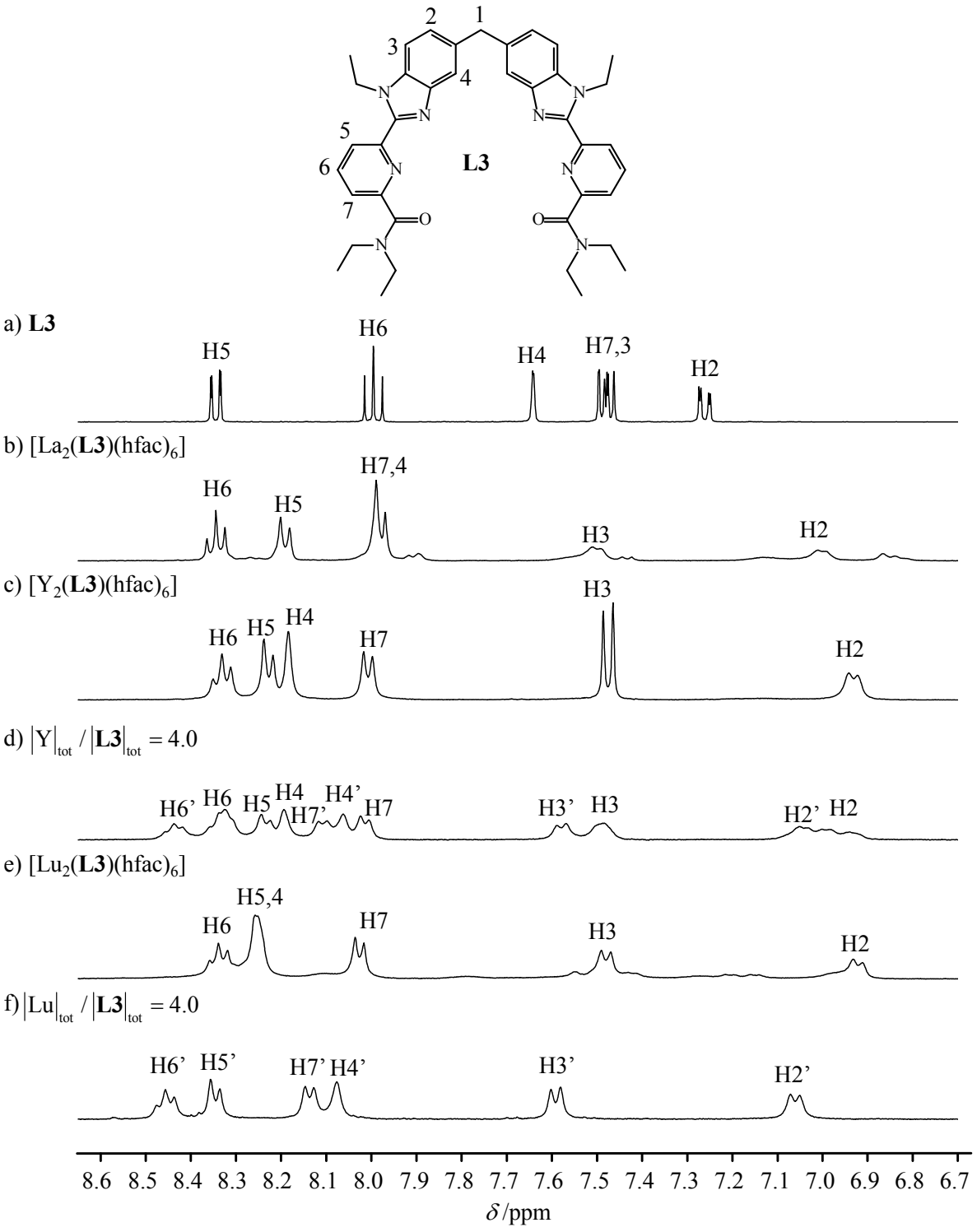

Figure S22 Aromatic parts of selected ^{1}H NMR spectra recorded during the titration of **L3** with [Ln(hfac)$_3$(diglyme)] in CD_3CN at 293 K. a) **L3**, b) La:**L3** = 2:1, c) Y:**L3** = 2:1, d) Y:**L3** = 4:1, e) Lu:**L3** = 2:1 and f) Lu:**L3** = 4:1. Protons with standard numbering correpond to those of [Ln$_2$(**L3**)(hfac)$_6$], whereas those marked are assigned to the dissociated complexes [Ln$_2$(**L3**)(hfac)$_4$]$^{2+}$ (see text).

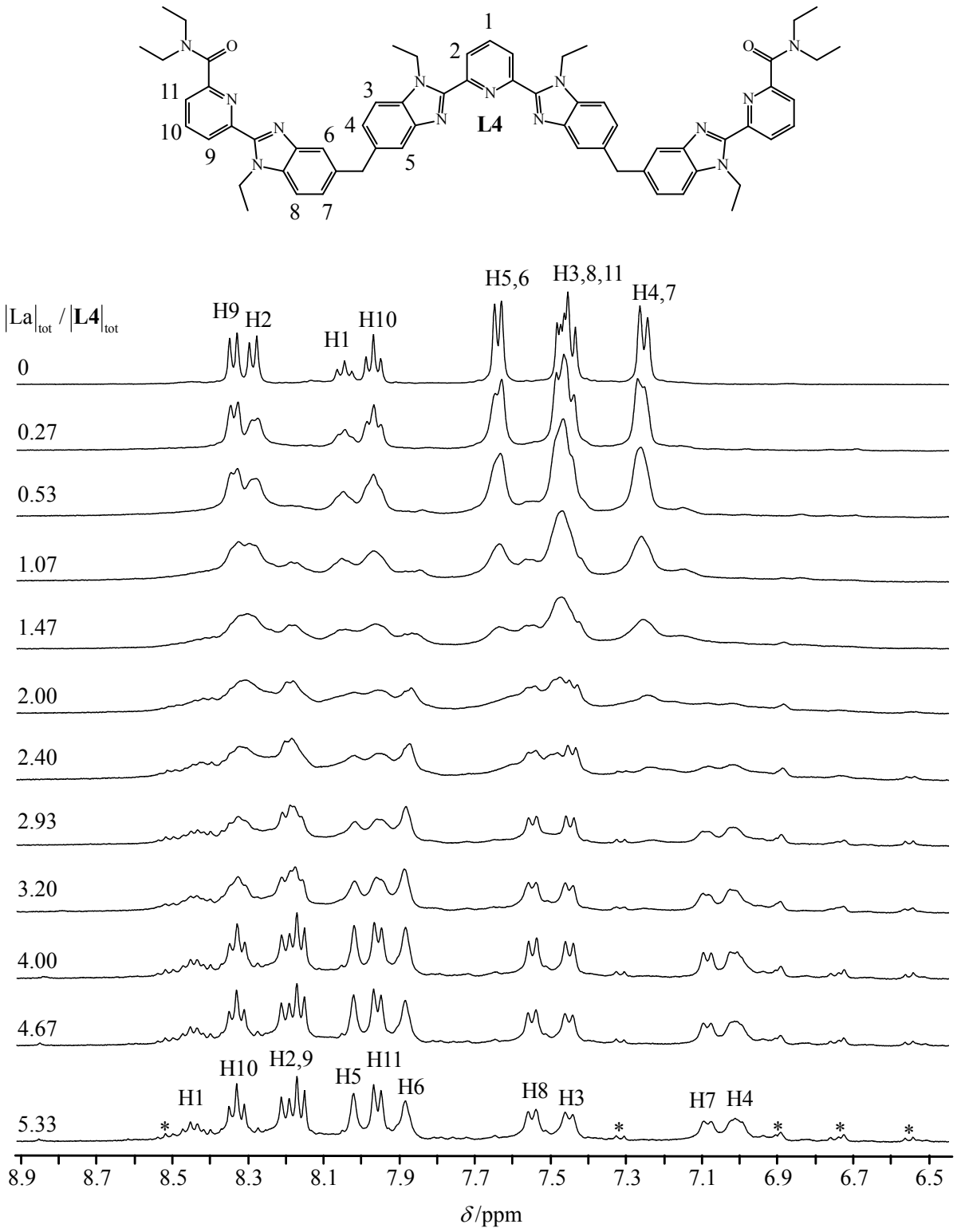

Figure S23 Aromatic parts of selected ^{1}H NMR spectra recorded during the titration of **L4** with [La(hfac)$_3$(diglyme)] in CD_3CN/CD_2Cl_2 (7:3) at 293 K. Protons with standard numbering correpond to those of [La_3(**L4**)(hfac)$_9$], whereas those marked with a star are assigned to traces of the double-stranded complex [La_3(**L4**)$_2$(hfac)$_8$]$^+$ (see text).

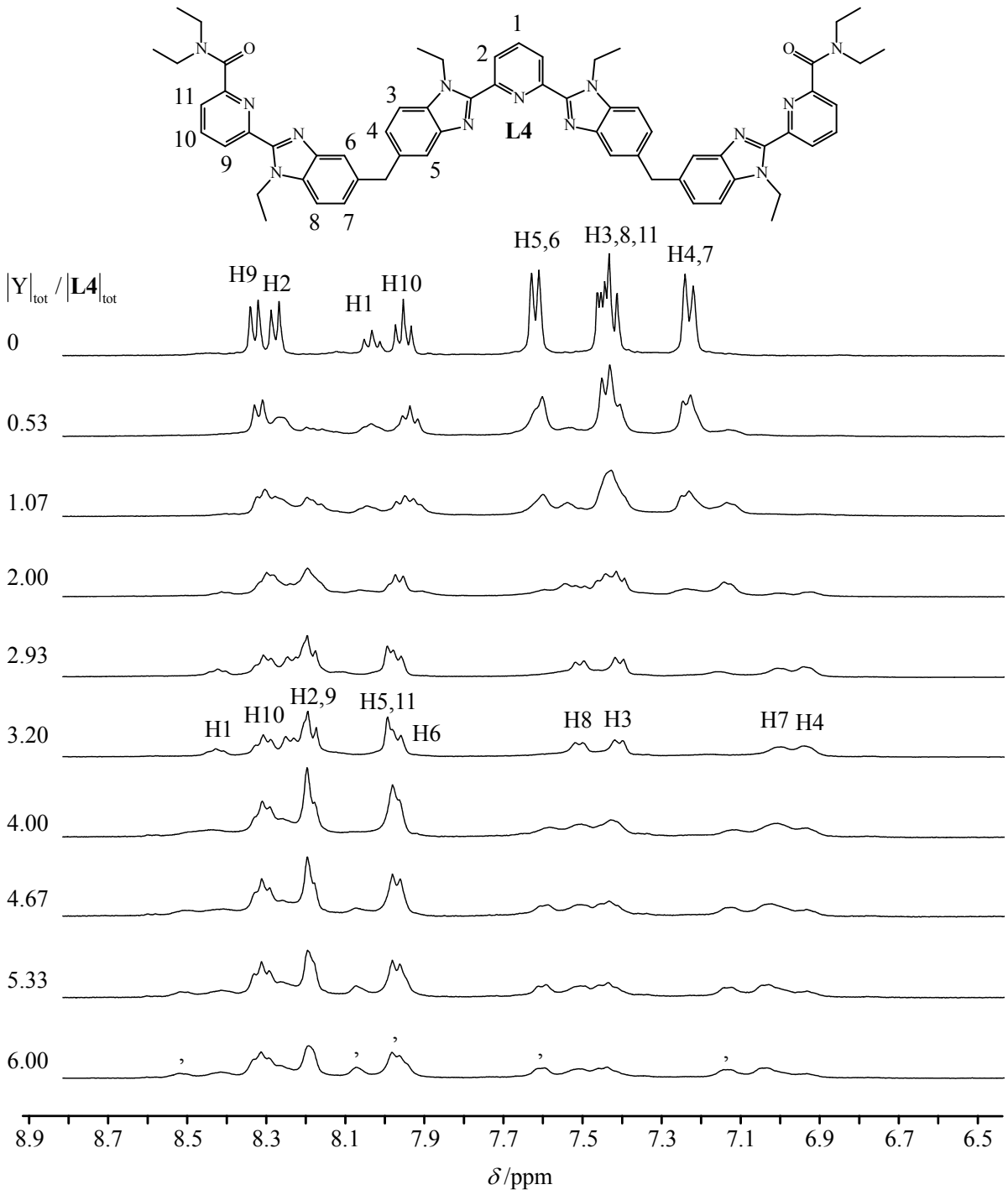

Figure S24 Aromatic parts of selected ^{1}H NMR spectra recorded during the titration of **L4** with [Y(hfac)$_3$(diglyme)] in CD_3CN/CD_2Cl_2 (7:3) at 293 K. Protons with standard numbering correpond to those of [Y_3(**L4**)(hfac)$_9$], whereas those primed are assigned to the dissociated complex [Y_3(**L4**)(hfac)$_8$]$^+$ (see text).

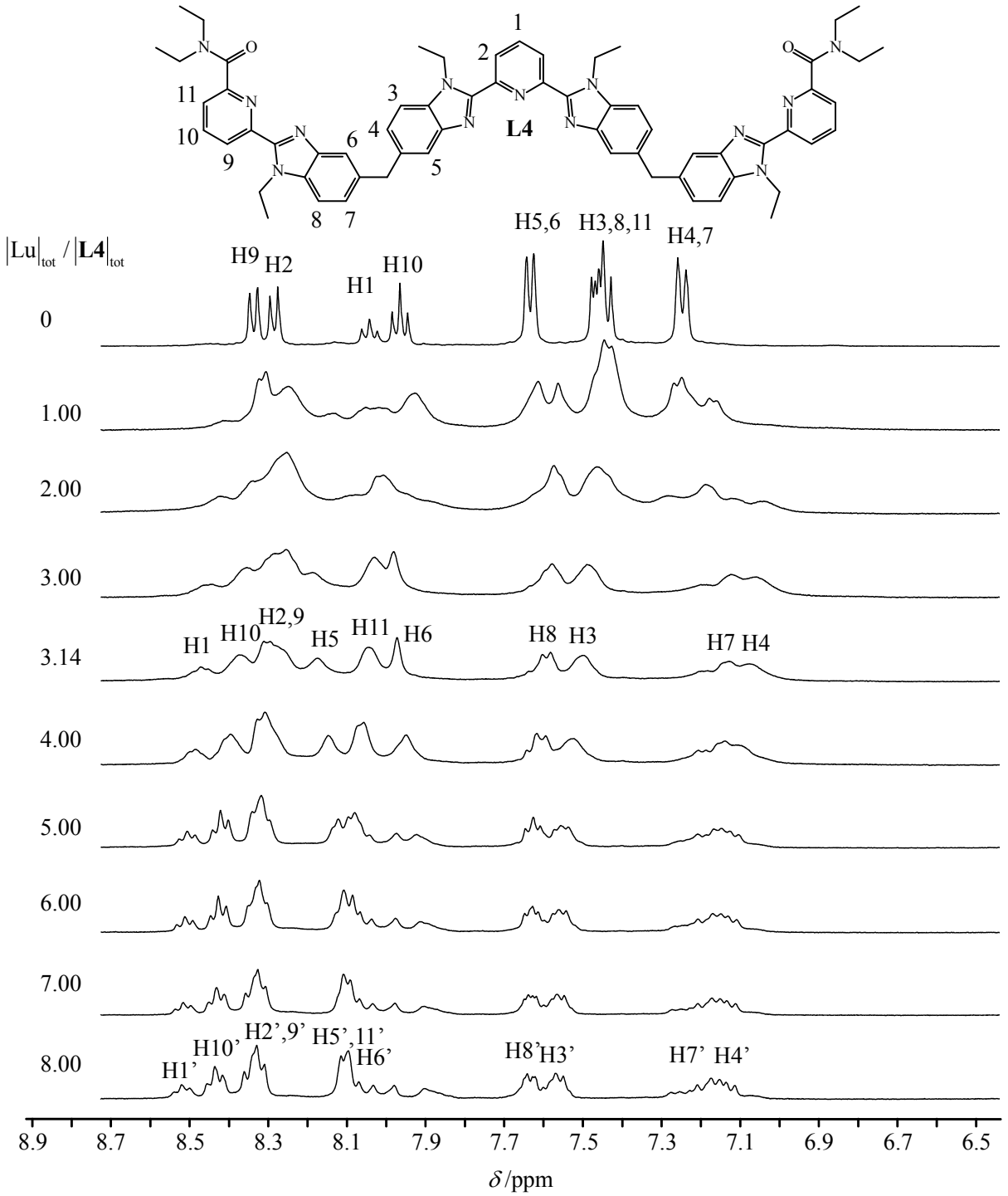

Figure S25 Aromatic parts of selected ^{1}H NMR spectra recorded during the titration of **L4** with [Lu(hfac)$_3$(diglyme)] in CD_3CN/CD_2Cl_2 (7:3) at 293 K. Protons with standard numbering correpond to those of [Lu$_3$(**L4**)(hfac)$_9$], whereas those primed are assigned to the dissociated complex [Lu$_3$(**L4**)(hfac)$_8$]$^+$ (see text).

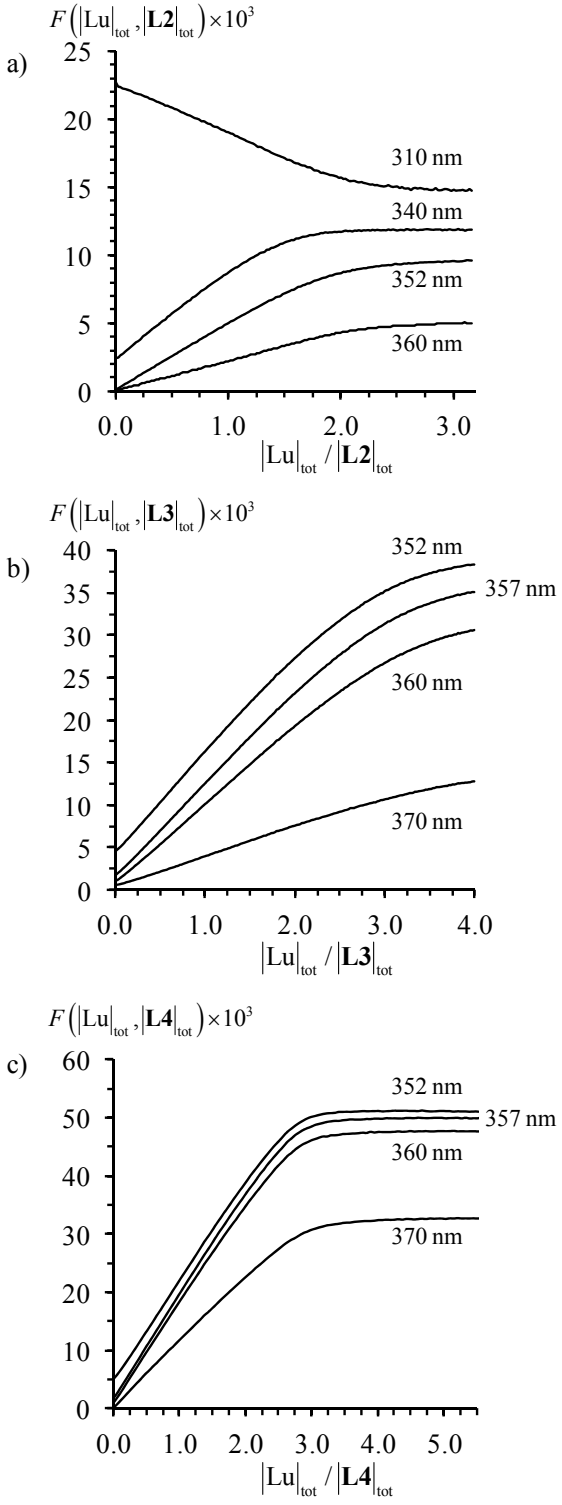

Figure S26 Variation of corrected molar extinction F (see appendix 3) at four different wavelengths observed during the spectrophotometric titrations of a) **L2**, b) **L3** and c) **L4** with [Lu(hfac)$_3$(diglyme)] (298 K, CH_3CN, total ligand concentration: 10^{-4} mol·dm^{-3}).

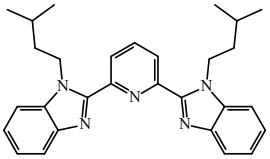

L1 + $[Ln(X)_3(CH_3CN)_3]$ $\overset{\beta_{1,1}^{Ln,L1}}{\rightleftharpoons}$ $[Ln(\mathbf{L1})(X)_3]$ + 3 CH_3CN (10)

Point groups:	C_{2v}	C_{3v}	C_{2v}	C_{3v}
σ^{ext}:	2	3	2	3
σ^{int}:	$2^2 3^4$	3^3	$2^2 3^4$	1
σ^{chiral}:	1	1	1	1

$$\Rightarrow \omega_{1,1}^{chiral} = \frac{1 \cdot 1}{1 \cdot 1} = 1 \qquad \omega_{1,1}^{Ln,\mathbf{L1}} = \frac{2 \cdot 2^2 \cdot 3^4 \cdot 3 \cdot 3^3}{2 \cdot 2^2 \cdot 3^4 \cdot 3^3} = 3$$

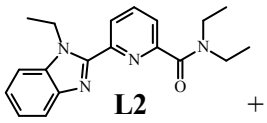

L2 + $[Ln(X)_3(CH_3CN)_3]$ $\overset{\beta_{1,1}^{Ln,L2}}{\rightleftharpoons}$ $[Ln(\mathbf{L1})(X)_3]$ + 3 CH_3CN (10)

Point groups:	C_s	C_{3v}	C_s	C_{3v}
σ^{ext}:	1	3	1	3
σ^{int}:	3^3	3^3	3^3	1
σ^{chiral}:	1	1	1	1

$$\Rightarrow \omega_{1,1}^{chiral} = \frac{1 \cdot 1}{1 \cdot 1} = 1 \qquad \omega_{1,1}^{Ln,\mathbf{L2}} = \frac{1 \cdot 3^2 \cdot 3 \cdot 3^3}{1 \cdot 3^3 \cdot 3^3} = 3$$

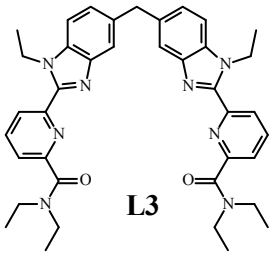

L3 + $[Ln(X)_3(CH_3CN)_3]$ $\overset{\beta_{1,1}^{Ln,L3}}{\rightleftharpoons}$ $[Ln(\mathbf{L3})(X)_3]$ + 3 CH_3CN (11)

Point groups:	C_{2v}	C_{3v}	C_s	C_{3v}
σ^{ext}:	2	3	1	3
σ^{int}:	3^6	3^3	3^6	1
σ^{chiral}:	1	1	1	1

$$\Rightarrow \omega_{1,1}^{chiral} = \frac{1 \cdot 1}{1 \cdot 1} = 1 \qquad \omega_{1,1}^{Ln,\mathbf{L3}} = \frac{2 \cdot 3^6 \cdot 3 \cdot 3^3}{1 \cdot 3^6 \cdot 3^3} = 6$$

L3 + 2 $[Ln(X)_3(CH_3CN)_3]$ $\overset{\beta_{2,1}^{Ln,L3}}{\rightleftharpoons}$ $[Ln_2(\mathbf{L3})(X)_6]$ + 6 CH_3CN (11)

Point groups:	C_{2v}	C_{3v}	C_{2v}	C_{3v}
σ^{ext}:	2	3	2	3
σ^{int}:	3^6	3^3	3^6	1
σ^{chiral}:	1	1	1	1

$$\Rightarrow \omega_{2,1}^{chiral} = \frac{1 \cdot 1}{1 \cdot 1} = 1 \qquad \omega_{2,1}^{Ln,\mathbf{L3}} = \frac{2 \cdot 3^6 \cdot \left(3 \cdot 3^3\right)^2}{2 \cdot 3^6 \cdot 3^6} = 9$$

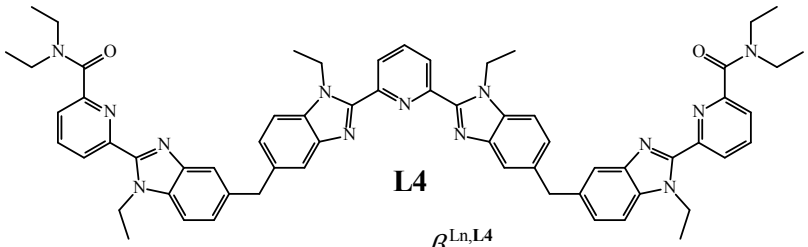

L4

$$\mathbf{L4} + [Ln(X)_3(CH_3CN)_3] \underset{}{\overset{\beta^{Ln,\mathbf{L4}}_{1,1,N_2O}}{\rightleftharpoons}} [Ln(\mathbf{L4})(X)_3] + 3\,CH_3CN \quad (12)$$

Point groups:	C_{2v}	C_{3v}	C_s	C_{3v}
σ^{ext}:	2	3	1	3
σ^{int}:	3^4	3^3	3^4	1
σ^{chiral}:	1	1	1	1

$$\Rightarrow \omega^{chiral}_{1,1} = \frac{1\cdot 1}{1\cdot 1} = 1 \qquad \omega^{Ln,\mathbf{L4}}_{1,1,N_2O} = \frac{2\cdot 3^4\cdot 3\cdot 3^3}{1\cdot 3^4\cdot 3^3} = 6$$

$$\mathbf{L4} + [Ln(X)_3(CH_3CN)_3] \underset{}{\overset{\beta^{Ln,\mathbf{L4}}_{1,1,N_3}}{\rightleftharpoons}} [Ln(\mathbf{L4})(X)_3] + 3\,CH_3CN \quad (12)$$

Point groups:	C_{2v}	C_{3v}	C_{2v}	C_{3v}
σ^{ext}:	2	3	2	3
σ^{int}:	3^4	3^3	3^4	1
σ^{chiral}:	1	1	1	1

$$\Rightarrow \omega^{chiral}_{1,1} = \frac{1\cdot 1}{1\cdot 1} = 1 \qquad \omega^{Ln,\mathbf{L4}}_{1,1,N_3} = \frac{2\cdot 3^4\cdot 3\cdot 3^3}{2\cdot 3^4\cdot 3^3} = 3$$

$$\mathbf{L4} + 2\,[Ln(X)_3(CH_3CN)_3] \underset{}{\overset{\beta^{Ln,\mathbf{L4}}_{2,1,N_2O}}{\rightleftharpoons}} [Ln_2(\mathbf{L4})(X)_6] + 6\,CH_3CN \quad (12)$$

Point groups:	C_{2v}	C_{3v}	C_{2v}	C_{3v}
σ^{ext}:	2	3	2	3
σ^{int}:	3^4	3^3	3^4	1
σ^{chiral}:	1	1	1	1

$$\Rightarrow \omega^{chiral}_{1,1} = \frac{1\cdot 1}{1\cdot 1} = 1 \qquad \omega^{Ln,\mathbf{L4}}_{2,1,N_2O} = \frac{2\cdot 3^4\cdot \left(3\cdot 3^3\right)^2}{2\cdot 3^4\cdot 3^6} = 9$$

$$\mathbf{L4} + 2\,[Ln(X)_3(CH_3CN)_3] \underset{}{\overset{\beta^{Ln,\mathbf{L4}}_{2,1,N_3}}{\rightleftharpoons}} [Ln_2(\mathbf{L4})(X)_6] + 6\,CH_3CN \quad (12)$$

Point groups:	C_{2v}	C_{3v}	C_s	C_{3v}
σ^{ext}:	2	3	1	3
σ^{int}:	3^4	3^3	3^4	1
σ^{chiral}:	1	1	1	1

$$\Rightarrow \omega^{chiral}_{1,1} = \frac{1\cdot 1}{1\cdot 1} = 1 \qquad \omega^{Ln,\mathbf{L4}}_{2,1,N_3} = \frac{2\cdot 3^4\cdot \left(3\cdot 3^3\right)^2}{1\cdot 3^4\cdot 3^6} = 18$$

$$\mathbf{L4} + 3\,[Ln(X)_3(CH_3CN)_3] \overset{\beta_{3,1}^{Ln,\mathbf{L4}}}{\rightleftharpoons} [Ln_3(\mathbf{L4})(X)_9] + 9\,CH_3CN \quad (12)$$

Point groups:	C_{2v}	C_{3v}	C_{2v}	C_{3v}
σ^{ext}:	2	3	2	3
σ^{int}:	3^4	3^3	3^4	1
σ^{chiral}:	1	1	1	1

$$\Rightarrow \omega_{1,1}^{chiral} = \frac{1 \cdot 1}{1 \cdot 1} = 1 \qquad \omega_{3,1}^{Ln,\mathbf{L4}} = \frac{2 \cdot 3^4 \cdot \left(3 \cdot 3^3\right)^3}{2 \cdot 3^4 \cdot 3^9} = 27$$

Figure S27 Symmetry numbers (σ) and statistical factors (ω) for the complexation of nine-coordinate $[Ln(X)_3(CH_3CN)_3]$ to **L1**-**L4** in acetonitrile (X = NO_3^- or $hfac^-$). For comparison purpose, we set that the weakly interacting water or diglyme molecules in the starting complexes are shifted by acetonitrile at 10^{-4} M. The somewhat arbitrary choice of an ideal C_{3v} symmetry for the starting lanthanide complexes is not crucial since each equilibrium refers to the same starting metal-containing entity.

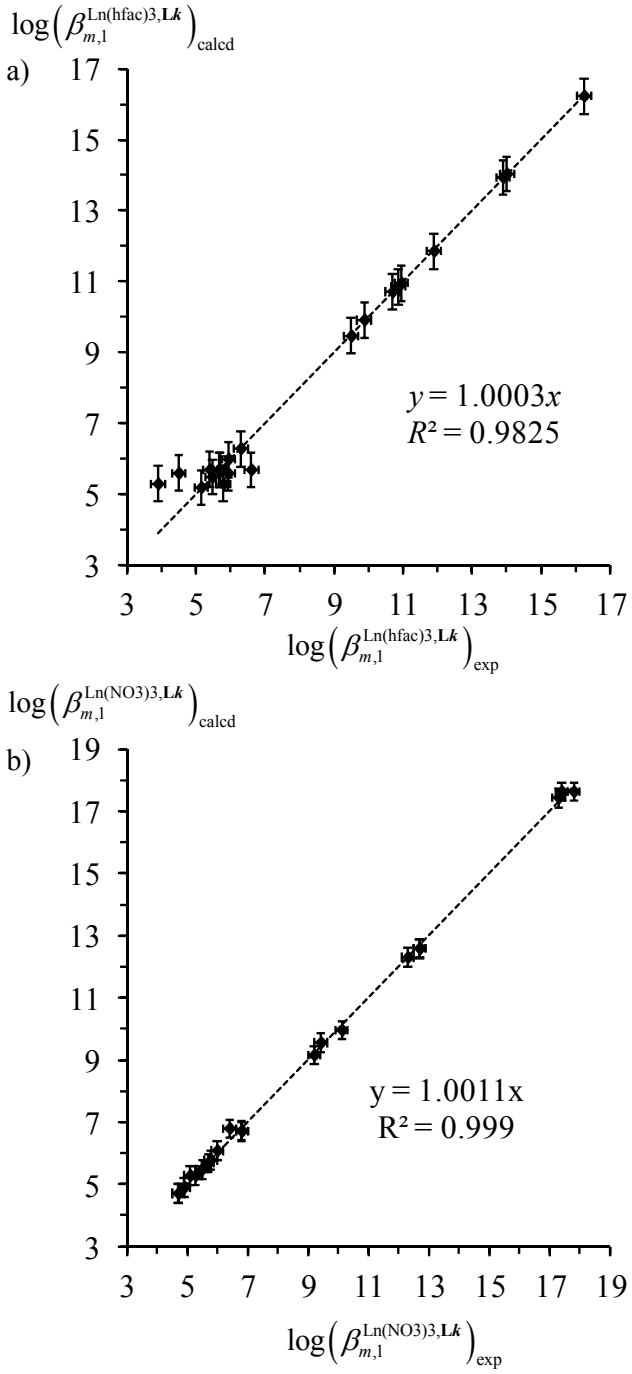

Figure S28 Cumulative experimental a) $\log\left(\beta_{m,1}^{\mathrm{Ln(hfac)3,L}\boldsymbol{k}}\right)_{\mathrm{exp}}$ and b) $\log\left(\beta_{m,1}^{\mathrm{Ln(NO3)3,L}\boldsymbol{k}}\right)_{\mathrm{exp}}$ (eqs 10-12) and calculated a) $\log\left(\beta_{m,1}^{\mathrm{Ln(hfac)3,L}\boldsymbol{k}}\right)_{\mathrm{calcd}}$ and b) $\log\left(\beta_{m,1}^{\mathrm{Ln(NO3)3,L}\boldsymbol{k}}\right)_{\mathrm{calcd}}$ (eqs 17-23) thermodynamic formation constants obtained for $[\mathrm{Ln}_m(\mathbf{L}\boldsymbol{k})(\mathrm{hfac})_{3m}]^{3m+}$ in CH_3CN at 298 K (Ln = La, Eu, Y; **L*k*** = **L1**-**L4**).

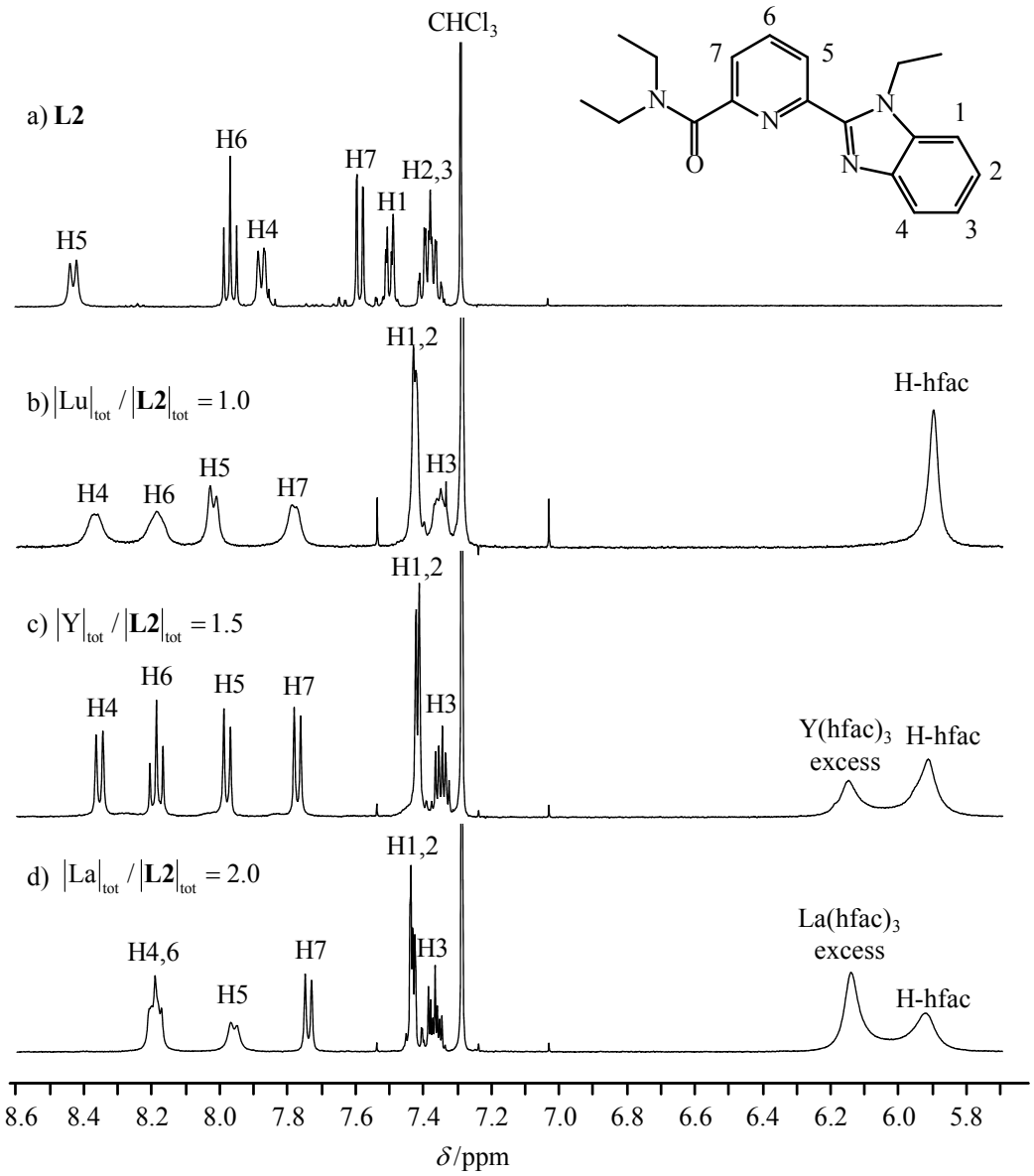

Figure S29 Selected ^{1}H NMR spectra recorded upon titration of **L2** with [Ln(hfac)$_3$(diglyme)] in $CDCl_3$ at 293 K. a) **L2**, b) Lu:**L2** = 1:1, c) Y:**L2** = 3:2 and d) La:**L2** = 2:1.

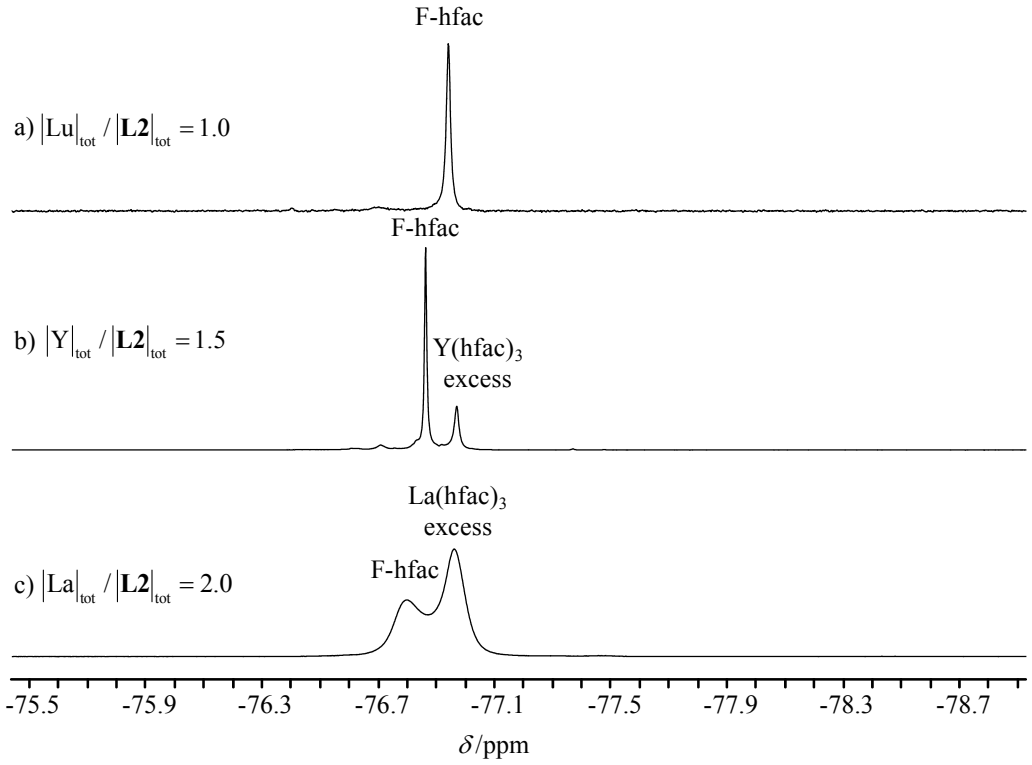

Figure S30 Selected ^{19}F NMR spectra recorded during the titration of **L2** with [Ln(hfac)$_3$(diglyme)] in $CDCl_3$ at 293 K. a) Lu:**L2** = 1:1, b) Y:**L2** = 3:2 and c) La:**L2** = 2:1.